Master Thesis CODEN:LUTMDN/(TMMV-5150)/1-127/2019

Vibration analysis for condition monitoring of mechanical presses

Julia Runesson

Lund 2019

DIVISION OF PRODUCTION AND MATERIALS
LUND INSTITUTE OF TECHNOLOGY, LUND UNIVERSITY

Abstract

In a world where the concept of just-in-time has been lifted outside of the manufacturing world and onto the market, the increasing demand of luxury wares like cars is accompanied only by tougher industrial conditions and no room for error. Loss of productivity and decrease in efficiency can be devastating to any manufacturing company in today's market climate. One of the largest causes of these issues is production downtime due to machine breakdown or unexpected failure.

To prevent such events from happening, Volvo Cars has decided to investigate the possibility of using vibration analysis for predictive maintenance and condition monitoring of presses used to manufacture sheet-metal car body components.

Although the concept of using vibration analysis for predictive maintenance is not new and the positive effects have been established, uses in complex machinery with intermittent cycles as mechanical presses have at the time of this thesis not been widely studied. This thesis aims to research if vibration analysis is a useable tool for predictive maintenance in mechanical presses and what information it might provide.

Vibration analysis is a wide field of technology and there are endless tools and methods to perform analysis. This thesis mainly focuses on the possibilities in using Power Spectral Density (PSD), Fast Fourier Transform (FFT) and statistical parameters like Root Mean Square (RMS) and Kurtosis. These are used in many applications and there are many companies that are familiar with implementing these tools, making them suitable to research.

After a thorough investigation of the use of PSD, FFT, RMS, and Kurtosis on the main components of the press crown and driving system, it is possible to conclude that vibration analysis is useable when using predictive maintenance on a press. Some configuration of PSD, FFT, and RMS gives the most benefits in detecting and analysing faults and issues. However, more data must be collected to establish when alarms must be issued to the maintenance crew and to build thorough models that provide enough information for making informed diagnosis and decisions based on vibration analysis.

Keywords: *Vibration analysis, Predictive maintenance, Condition monitoring, Mechanical press, Press maintenance, PSD, DFT/FFT, RMS, Kurtosis*

Sammanfattning

I en värld där begreppet ”just-in-time” är lika relevant på marknaden som inom tillverkningsindustri så kommer en ökande efterfrågan på lyxvaror som bilar med allt tuffare krav inom industrin och mindre utrymme för misstag.

Produktivitetsförlust och nedsatt effektivitet kan vara förödande för vilket tillverkningsföretag som helst i dagens marknadsklimat. En av de största orsakerna till dessa problem är oplanerade stillestånd orsakade av maskinhaveri. För att förhindra att detta inträffar har Volvo Cars valt att undersöka möjligheten att använda vibrationsanalys för prediktivt underhåll på de pressar som används för att tillverka plåtkomponenter till bilar.

Att använda vibrationsanalys för prediktivt underhåll är inget nytt koncept och de positiva effekterna är redan bevisade, men användningen i komplext maskineri med intermittent verkan, som mekaniska pressar, har i skrivande stund inte blivit studerat i detalj. Detta arbete ämnar undersöka om vibrationsanalys är användbart för prediktivt underhåll av mekaniska pressar och vilken sorts information analysen kan förse.

Vibrationsanalys är ett brett område av teknologi och det finns oändligt med verktyg och metoder att använda för analys. Detta arbete fokuserar på möjligheten att använda *Power Spectral Density* (PSD), *Fast Fourier Transform* (FFT) samt statistiska mått som kvadratiskt medelvärde (RMS) och kurtosis. Dessa verktyg används i ett flertal applikationer och implementationen är beprövad, vilket gör det passande att vidare undersöka dess användbarhet i även denna tillämpning.

Efter noggrann granskning utav användningen av PSD, FFT, RMS och kurtosis för analys av huvudkomponenterna i pressens krona och drivsystem så kan det konstateras att vibrationsanalys är ett användbart verktyg för prediktivt underhåll av mekaniska pressar. Någon konstellation av PSD, FFT och RMS ger störst fördelar i att upptäcka och diagnostisera fel och problem. Dock måste mer data samlas in och analyseras för att kunna sätta passande gränser för då alarm ska utfärdas till underhållspersonalen. Samt för att kunna bygga utförliga modeller som tillhandahåller tillräcklig information för informerande beslut och för diagnostisering genom vibrationsanalys.

Nyckelord: *Vibrationsanalys, Prediktivt underhåll, Tillståndsövervakning, Mekanisk press, Press-underhåll, PSD, DFT/FFT, RMS, Kurtosis*

Acknowledgements

This master thesis was conducted for the division of Production and Materials Engineering at Lund University in collaboration with Volvo Cars, Olofström.

I would like to thank my supervisor Toini Sjöqvist for taking me under her wings and taking the time (more than once) to reason with me about the scope of this thesis. Thank you for making time for me in your busy schedule.

I would also like to give thanks to my supervisor Christina Windmark for teaching me that writing should be a creative process and for helping me finalize this report. Thank you, Christina.

A huge thank you to my supervisor Oleksandr Gutnichenko for helping get started with the analysis. I do not know what I would have done without you.

Thank you, Klas Jakobsson, for showing me the positioning of the sensors in real life and explaining how the press operates.

Thank you, Daniel Stenmark, for introducing me to the current software and helping me with the data extraction.

Thank you to all the wonderful people at Volvo, it has been a pleasure meeting all of you.

Lastly a special thanks to my wonderful parents Joakim and Anna-Carin and my partner Herman. Your emotional support has been invaluable.

Julia Runesson, Karlshamn

Ger pressar dig bra vibrationer?

Idag är allt från kaffemaskiner och gräsklippare till krutpistoler och bilar uppkopplade och kan närsomhelst ge oss en statusrapport genom bara ett par klick i en app. Vi kan med mobilen kolla bilens bränslenivå, geografiska position eller om vi glömt att låsa på väg in från parkeringen. Så varför skulle inte statusen på utrustningen som används för att tillverka bilen vara lika enkel att kontrollera?

Tillståndsövervakning är en viktig del av prediktivt underhåll. Sensorer av olika slag används för att samla in data om utrustningen som annars skulle gå förlorad. Genom att jämföra nya och historiska data kan försämrade tillstånd och fel upptäckas i god tid innan följdfel och långa stillestånd blir ett faktum.

Vibrationsövervakning har länge använts för att bestämma tillståndet på enklare utrustningar. Med goda resultat bör tilläggas. Användningen av vibrationer för att bestämma tillståndet på komplex utrustning är däremot inte lika beprövat och är det ämnet som diskuteras och prövas i examensarbetet ”*Vibration analysis for condition monitoring of mechanical presses*”.

Volvo Cars är allmänt kända för att tillverka bilar som ligger i framkant av innovation och säkerhet som gynnar inte bara förare och passagerare men även de som befinner sig utanför bilen. Utöver uppkopplade bilar och oöverträffad säkerhet så levererar Volvo bilar som sannerligen är en fröjd för ögat. Med bilar som är designade inte bara för att attrahera blickar, skapa körglädje eller göra bilresan till mataffären mindre riskfylld men också för att tillverkas i stort antal och i hög takt. Karosseridetaljerna tillverkas genom pressning i den lilla pittoreska staden Olofström i södra Sverige. Härifrån levereras plåtdetaljer till hela världen ingen ensam detalj är viktigare än någon annan i slutmonteringen av en sprillans ny V90 eller XC40.

Det föga förvånande att efterfrågan på Volvos bilar är hög men det sätter även högt tryck på fabriken i Olofström att pressa fram detaljer i ett jämnt tempo. Fabriken omfattar totalt 27 presslinjer med 5–6 pressar vardera. Om någon av dessa pressar skulle haverera så kan det resultera i kostsam förlust av viktig produktionstid och genom tillämpning av prediktivt underhåll kan denna risken reduceras. Det är här vi återkommer till komplex utrustning och tillståndsövervakning. En press är komplex på det viset att det finns många variabler som på olika sätt påverkar varandra och det är därför inte självklart att vibrationsövervakning kan tillämpas med samma goda resultat som på en enklare utrustning.

Av examensarbetet ”*Vibration analysis for condition monitoring of mechanical presses*” så kan det konstateras att det visst går att tillämpa vibrationsövervakning på en press och på så sätt göra tillverkningen av karosseridetaljer lika tillförlitlig som den där kaffemaskinen som räddar så många av oss varje morgon.

Julia Runesson, 2019

Table of contents

1 Introduction

1.1 Company description

Volvo car group (Volvo Cars) is a manufacturer and developer of passenger cars [1]. The company was founded in Gothenburg, Sweden and began manufacturing in 1927. Today Volvo Cars is an international actor working and delivering award-winning cars worldwide.

Volvo Cars' aim is to continue being global leaders in automotive safety, electrification, and autonomous drive and are already offering a wide range of hybrid cars. 38 000 employees worldwide help drive the development of Volvo Cars forward and into the future.

With sales in over 100 countries, the company sold 642 000 cars in 2018 that were all developed, manufactured and assembled within the company's worldwide business.

Manufacturing plants are situated in Sweden, Belgium, USA and China. The manufacturing in these plants is characterized by attention to quality, safety and environmental responsibility [1].

1.2 Background

Most of the metal body components that are used in cars made by Volvo are manufactured by means of sheet metal forming in Olofström, Sweden. This includes for example doorframes, exterior doors, and several different beams; all crucial to the final car produced. Every car body component requires several dedicated press tools to be manufactured. These press tools are made to fit a certain line of machinery with little to no flexibility.

Mechanical presses are often used for mass production making standstills expensive due to loss of productivity. As spare parts are often large and non-standard, standstills due to unexpected breakdown tend to lengthen in time as spare parts are being delivered. This project investigates the use of vibration analysis in order to catch the need for maintenance of a press before anything fails and causes lengthy downtimes. Having vibration analysis as a complement to ocular inspections that are carried out by maintenance may help catch hidden faults before they lead to failure.

During 2018 accelerometers were placed on several different but corresponding positions/components of two presses in the same press line. The placement is presented in 4.1. Vibrations were recorded during certain times with the presses being in three different conditions:

- Bad condition (in need of refurbishment)
- Decent condition
- Good condition (newly refurbished)

However, all three conditions were not recorded in both presses respectively. Conditions 'bad' and 'good' were recorded in one press and the other press has only been recorded in what is assumed 'decent' condition. Because of this, the data from the two presses will have to be compared to see if the same vibrational behaviour can be observed in similar components but in two different machines.

During the analysis of the data, suitable segments of the press cycle have been cropped out to make the signal more reliable and minimize errors due to aperiodic impulses. Furthermore, all measurements were recorded while manufacturing the same type of detail to eliminate variations caused by running conditions.

1.3 Objectives

This project aims to further investigate the possibility of using vibration analysis as a complement to ocular inspection for predictive maintenance and condition monitoring on mechanical presses used for sheet metal forming.

Via analysis of collected vibration data the following is discussed:

- Can vibration analysis be used for predictive maintenance of a mechanical press in the sense of fault detection and fault analysis (explained further in 2.4)?
- Which type of analysis provides necessary information about the condition of different components?
- How to interpret collected vibration data in an analysis.
- How much information will vibration analysis provide about the condition?
- Is vibrational information exchangeable between corresponding components on different equipment?

The possibility of using machine learning to predict the condition of the press will also be briefly examined.

In addition to answering these questions, this thesis explains some of the basics of vibration analysis and machine learning so that the reader can grasp the content of this thesis without any prior knowledge within the field. While also providing foundational knowledge for future thesis works.

1.4 Delimitations

The focus of this thesis is to understand if and how vibration analysis might be useable in condition monitoring of mechanical presses. Both detection of faults and diagnosis is discussed. The methods used for analysis are chosen based on their computational simplicity and that they are available in the software presently used in this application at Volvo Cars.

For most of the analysed components the condition at the time of measurement is not known. Because of this, conclusions regarding condition and/or diagnosis of both past and present measurements are only assumptions and will have to be confirmed to make reliable conclusions.

The prospect of using machine learning for implementation will be briefly discussed but the subject of data processing or -handling needed to create an automatic condition monitoring system will not be discussed in detail.

1.5 Resources

Resources for this thesis have been available in the form of:

- Data available through accelerometers previously mounted on several deliberately and professionally chosen positions on the concerned equipment.
- Help to get going with data acquisition and using the present software by a representative from the company that performed initial vibration analysis and implementation.
- Student license version of Matlab for analysis.
- Executive supervisor with extensive experience with vibration analysis and machine learning.

1.6 Confidentiality

Volvo Cars has decided that the information found in thesis is to be regarded as general knowledge and is not viewed as confidential company information.
However, …

- The make and exact configuration of the presses involved is not disclosed.
- Nor is the exact positioning of the accelerometers which is only described generally.
- Current maintenance practices are not described in detail.
- Exact dates and times of the measurements is not included in this thesis.
- Neither is the Matlab code.

1.7 Target audience

The target audience of this master thesis is first and foremost the people implementing technologies like vibration analysis and other means of data collection/analysis while working with mechanical presses and other complex machines. This thesis also aims to act as an initial look into using vibration analysis for those working with maintenance at Volvo in Olofström.

1.8 Disposition

- **Introduction** *Gives a background to the company, what has previously been done within the area at the company and what the company stands to gains with this thesis. This chapter also contains the outlining objectives and delimitations as well as a description of the target audience and the confidentiality applied to the report.*

- **Theoretical background** *Gives the reader a theoretical background on predictive maintenance and why it is important. Also discussing the tools and methods used for vibration analysis and how to interpret the result. Parts of the theoretical background may provide important information for implementation and future work.*

- **Similar applications and implementation** *This chapter accounts some similar applications of vibration analysis that have been successfully implemented. The basics of machine learning and similar applications of vibration analysis with machine learning is also discussed.*
- **Data analysis** *Results of the analysis and further assumptions are simultaneously presented and discussed in this passage. This chapter also contains a description of the analysis method applied in this thesis.*
- **Discussion** *Concludes the most important take-aways of the analysis while thoroughly discussing the objectives formulated in the introduction.*
- **Conclusion** *Concludes the work done in this thesis and gives recommendations on future actions and thesis work.*
- **Appendix A** *Shortcut guide to diagnosing common faults through spectral analysis*

2 Theoretical background

2.1 Anatomy of a mechanical press

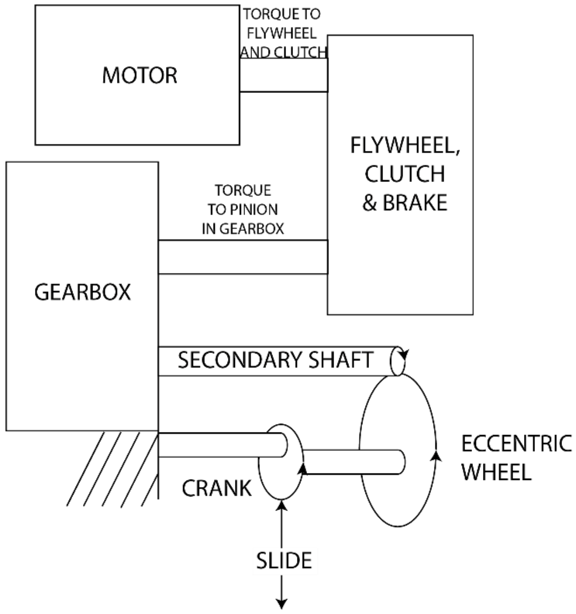

Figure 1. Schematic overview of the driving element of a mechanical press (minus tooling) [2]

The principal of a mechanical press is basic. Rotating motion is transferred from a motor through a series of shafts and gears finally generating a linear up-and-down motion of the slide. The press tool is split in two halves, a top and a bottom, the top half moves up and down with the slide and the bottom half is held in place on top of the press bed.

Figure 1 is a schematic overview of what a mechanical press with an eccentric wheel may look like. When the tool goes down the clutch is engaged and the motor brings torque to a flywheel, often done via a pulley. The flywheel is used to conserve and balance kinematic energy and is what helps the slide go upwards again. The flywheel is controlled by the clutch and a break that stops the press at the top where it pauses between strokes. During the paus the clutch is not engaged, and the motor runs freely [2].

Torque is then lead from the flywheel/clutch to the small gear, the pinion, of the gearbox which then exchanges torque to a larger gear. The larger gear is connected to a shaft called the secondary shaft. The secondary shaft exchanges torque to an eccentric wheel that controls the crank motion of the crank shaft. The crank brings motion to the connecting rod that makes the slide go up and down. Some of the shafts use bearings or bushings to be able to rotate without resistance within their fastenings, making the process more stable and more energy efficient [2].

Oftentimes there are two shafts and connecting rods that control the slide in parallel, this helps keep the slide aligned throughout the stroke [3].

One up-down-up motion of the slide equals one press stroke and one 360 degrees rotation of the crank that controls the motion of the connecting rod. Often one stroke is counted as 360 degrees with 180 degrees being when the press is in its' lowest position, the bottom dead centre (BDC) [4].

The force and impact on the tooling and machinery is largest just before-to the BDC of the stroke when the tool is in engagement causing high peaks of vibrations throughout the equipment [4].

Mechanical presses are complex in nature. All components in the machinery will in some way affect each other and the resulting product. As the number of variables large, any analysis of the machinery will in turns be complex if the number of variables is not reduced in any way possible.

2.2 Predictive maintenance

There are different models for planning when and how maintenance is performed. One method is "run-to-failure" which is a method that allows the equipment to fail before performing any maintenance. This requires fast repairs and readily available spare parts in order not to impact productivity [5]. Another method is preventative maintenance which implies that maintenance is scheduled after a certain number of operating hours. Planning using this method may result in equipment being replaced despite being fully operably or in unexpected failure prior to planned maintenance. A third model is proactive maintenance which means that sources of failure are redesigned or designed out to prevent the same sort of failure to be repeated. Using this model, maintenance is often scheduled in a way like preventative maintenance. The model is hard to use efficiently when failures are caused by critical components that most often fail from wear [5] [6].

Predictive maintenance is a fourth option that differs a bit from run-to-failure and preventative/proactive maintenance as the method requires regular and direct monitoring of the equipment [5]. Using careful condition-monitoring of concerned equipment to identify trends that indicate wear, like strange noises, then maintenance can be planned accordingly and be performed when most convenient. Using data-driven methods for condition-monitoring also reduces the need for physical and ocular inspections and helps pinpoint specific faults which helps make the maintenance-process quicker and more efficient. Critical spare parts with long delivery times can be ordered ahead of time without risking unnecessary tied-up capital. Predictive maintenance may also help extending intervals between repairs [5] [6].

There are several different ways of monitoring the condition of equipment. Vibration monitoring, acoustic emission analysis, oil analysis, corrosion monitoring, process parameter/performance monitoring, thermography, tribology, and visual inspection are often used as they are all non-intrusive. Vibration monitoring is most common and an effective tool to use with mechanical equipment [5] [6].

Predictive maintenance has been found to reduce direct costs for maintenance by 20-25% while also increasing productivity by minimizing downtimes and often even improving overall product quality [5, p. 5]. To get the optimum result with predictive maintenance the method must be expanded to include more than condition-monitoring. It must be applied on a larger scale.

In *An Introduction to Predictive Maintenance*, the author Mobley states predictive maintenance may help optimize total plant operation; “Including predictive maintenance in a comprehensive maintenance management program optimizes the availability of process machinery and greatly reduces the cost of maintenance. It also improves the product quality, productivity, and profitability of manufacturing and production plants.” [6, p. 5].

2.3 Vibration analysis

Rotating machine element create vibrations that are a function of machine dynamics. Vibration analysis enables the ability to tell if there is a misalignment or unbalance of an axle, deteriorating or defective bearings and gears or if vibrations in certain machine elements are amplified by resonance. This is done through the analysis of amplitudes at certain frequencies or trends in statistical measures. Analysis of trends in data may also reveal improper maintenance practices such as poor installation and replacement of bearings or poor alignment of rotors and shafts [7].

Vibrations are physical quantities that be either periodic like a pendulum, or stochastic (random) like the vibrations of a car driving on a gravel road [8].

Vibrations in mechanical components are of a non-stationary stochastic nature. This means that the signal characteristic may be changing and drifting over time and cannot always be expected to follow a statistical pattern [9].

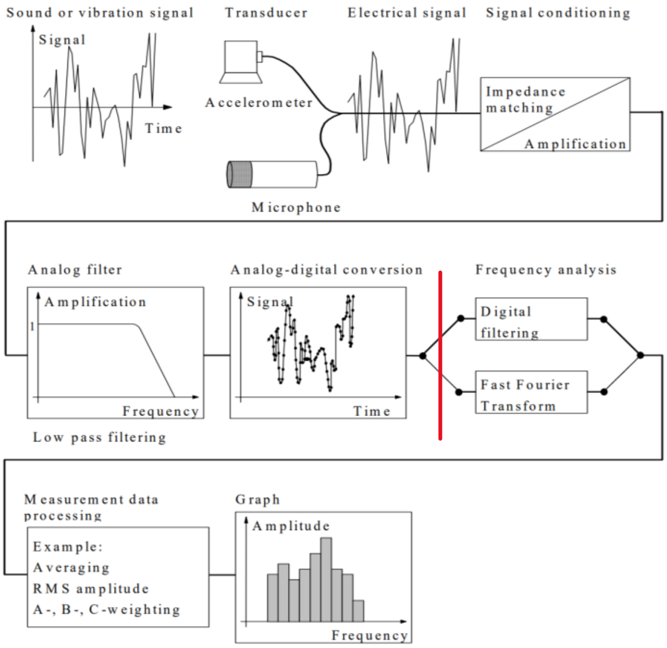

Figure 2. The vibration analysis process using sensors. [7]

Monitoring vibrations requires the use of sensors and most often accelerometers are used. The vibration analysis process using sensors is described in Figure 2 above. This thesis will focus around the last 3 steps, found after the red line in Figure 2:

- Frequency analysis,
- measurement data processing,
- and graphing (/making plots) [7].

2.3.1 Time-domain analysis

Time-domain analysis is based on different statistical parameters connected to the amplitude of the displacement, velocity or acceleration of the vibrations. Parameters like minimum value, maximum value, mean value, variance, standard deviation and root-mean-square (RMS) are called dimensional parameters and are related to operating conditions. Parameters like kurtosis (the number of transients in the signal), shape factor, peak value (the maximum level recorded during the concerned interval of time) and crest factor (the ratio between RMS and peak value) are called non-dimensional and might be more accurate for abrupt failure diagnosis or analysis of strong transient impulses [10, pp. 26-34].

Vibration data in the time-domain is plotted as overall vibration amplitude versus time. Vibrations can be analysed with respect to displacement, velocity and acceleration, all directly dependent on the time series. Analysis of these parameters are of varying importance to different failure modes but are all of relevance when deciding vibration amplitudes [7]. This type of analysis is useful in studying changes in conditions since historical data collected at the same running speed and load is directly comparable. However, this makes the method sensitive to variations in running speed and load. Also, this type of analysis is difficult to use for close-detail analysis as the amplitude of all data in the signal is summed up and will represent the total amplitude for a given interval of time [6, p. 118].

Analysis of displacement may be important when looking at vibrations in a brittle structures and materials like cast iron that are sensitive to crack-formation [7]. The root-mean-square (RMS) is a measure of the energy content of the vibrations which in some cases is an important angle of analysis. Measurement of acceleration is equal to measurement of force. High forces on bearings and bushings may lead to faults like insufficient lubrication that may cause failure. A load of 10% more than the bearing's designed static load may overtime cause dynamic forces that lead to failure [7].

The range of frequencies in the signal may otherwise help determine if acceleration, velocity or displacement should be used for analysis. Recommendations for different ranges of frequencies can be found in Table 1 below. This is also applicable to frequency domain analysis [7].

Table 1. Recommendation of parameter for analysis corresponding to range of frequency. [7]

FREQUENCY RANGE	RECOMMENDED PARAMETER
<10 HZ	Displacement
10-1000 HZ	Velocity
>1000 HZ	Acceleration

2.3.1.1 Root Mean Square (RMS)

As previously mentioned, the Root Mean Square (RMS) is related to the energy content of the signal. An increase of RMS indicates that the overall vibration level has increased, and a defect might be present [7].

The International Standards Organisation (ISO) has developed a standard regarding machine vibrations in non-rotating parts like bearings on for example motors: SS-ISO 10816-3 *"Mechanical vibration – Evaluation of machine vibration by measurements on non-rotating parts - Part 3: Industrial machines with nominal power above 15 kW and nominal speeds between 120 r/min and 15 000 r/min when measured in situ"* [11].

SS-ISO 10816-3 covers criteria for assessing machine vibrations caused by the machinery itself and not outside sources. Based on the amount of information accessible about the actual condition of the machine two different criterion can be used. First criterion requires thorough knowledge of the condition and considers the magnitude of observed vibrations. Second criterion requires only a well-defined baseline magnitude and considers the change of magnitudes observed.

When applying the first criterion the standard divides vibration severity into four different zones A-D:

- Zone A: Levels of vibrations of newly commissioned machines.
- Zone B: Levels of vibrations considered acceptable for long-term operation.
- Zone C: Levels of vibrations considered unacceptable for long-term operation. Machinery may be run within this zone a limited period before taking remedial action.
- Zone D: Levels of vibrations considered harmful to the health of the machinery. [11]

When using the second criterion all machines should be regarded individually, and the base level-amplitude of vibration should be decided separately for each machine. However, SS-ISO 10816-3 provides numeric guidelines for the zonal limits based on the machine characteristics. Medium-sized machines with rated power above 15 kW up to and including 300 kW and electrical machines with shaft height 160 mm $\leq H < 315$ mm and rigid support (like the motors regarded in this thesis) have the following limits:

- Limit zone A/B: RMS displacement = 22µm, RMS velocity = 1,4mm/s

- Limit zone B/C: RMS displacement = 45µm, RMS velocity = 2,8mm/s
- Limit zone C/D: RMS displacement = 71µm, RMS velocity = 4,5mm/s [11]

SS-ISO 10816-3 provides recommendations for setting the alarm- and trip-level (when immediate action should be taken to prevent serious damage) for both criterion (specifics can be found in [11, p. 8]).

The limits should be adjusted according to the vibration levels of the concerned equipment and the corresponding characteristics. When monitoring new or newly repaired machinery, the limits should be revised. [11]

2.3.1.2 Kurtosis

Kurtosis is a non-dimensional statistical measurement of the number of outliers in a distribution. In terms of vibration analysis kurtosis is corresponding to the number of transient peaks. A high number of transient peaks and a high kurtosis-value may be indicative of wear. For example, a good bearing with no flaws that cause impulses to the signal will have a kurtosis-value ~3 and in general a kurtosis-value above 4 is a sign of a bad condition [12, pp. 499-500].

Kurtosis is not sensitive to running speed or load, however, as a fault merges from a localized fault to a distributed fault, the impulsive content of the signal will decrease, causing the kurtosis-value to go down. In other words, the effectiveness of kurtosis is dependent on the presence of significant impulsiveness in the signal and is therefore most effective in finding newly sprung issues that have not yet subsided into distributed damage [13, pp. 499-500].

2.3.2 Frequency domain analysis

Frequency domain (or spectral) analysis is used to investigate the level of vibrations at narrow bands of frequencies, unlike time domain analysis and measures like for example RMS that regard the overall vibration level across a broad band of frequencies. This makes it possible to distinguish between different sources of vibrations and the characteristic frequencies of different defects. The possibility to differentiate between both different components and different faults will help decrease the amount of measuring equipment and time needed to diagnose faulty machinery [13].

The frequency-domain is an important angle of analysis. The frequency might explain what the issue is, and the amplitude will explain the severity. As a fault develops the amplitude of the frequency associated with the fault will increase. Although the level of this certain frequency is increasing, the overall vibration level or maximum peak level might be unaffected with regards to the time-domain. Using the frequency-domain will in this case make it possible to detect and possible diagnose the fault earlier [14]. The basis of frequency domain analysis is illustrated in Figure 3 below.

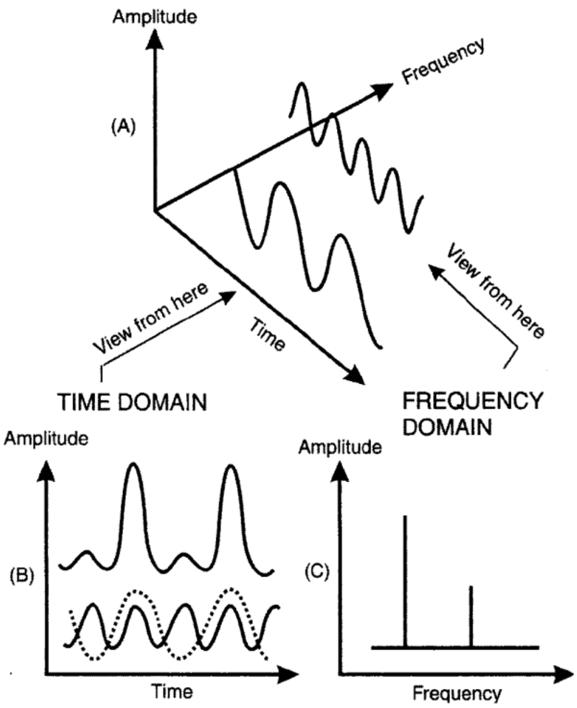

Figure 3. Illustrated explanation of the view of vibration in the time-domain (bottom left) and the frequency-domain (bottom right) [5, p. 56]

2.3.2.1 Fourier transform

The *Discrete Fourier Transform* (DFT) is used to transform analog signals from the time-domain to the frequency-domain. DFT will separate the various frequencies and amplitudes that make up a discrete signal (signal that is limited in length/time). Commonly when speaking of Fourier transforms, the *Fast Fourier transform* (FFT) is mentioned. FFT is an algorithm used to calculate the DFT of a signal and is popular due to calculation speediness. The length of the FFT is a power of two (N^2) and this property is what makes the FFT especially 'fast' [15, pp. 130-132].

The Root Mean Square (RMS) amplitude between two frequencies f_1 and f_2 can be calculated as:

$$\sqrt{2\sum_{f_1}^{f_2}|X(f)|^2} \qquad \text{(Eq.1) [16]}$$

Where *X(f)* is the absolute value of the complex components of the DFT at each spectral line (/frequency *f*).

If one wishes to calculate the RMS of the entire spectrum the frequency limits applied should be $f_1 = 0$ and $f_2 = fs/2$, where *fs* is the signals sampling rate [16].

2.3.2.2 Power Spectral Density

The Power Spectral Density (PSD) is a kind of histogram that represents how the power of a signal is distributed over a spectrum of frequencies. PSD is calculated as the mean-square average of the FFT over a band of frequencies and will therefore have a unit like e.g. g^2/Hz (when the amplitude of FFT is in g's) [17].

PSD may be useful in fault detection in condition monitoring of complex machinery. RMS and kurtosis are traditionally used for fault detection but are only truly reliable for simple components so a better option might be using PSD for spectral comparison or -trending [13].

Spectral comparison uses a baseline power spectral density that has been taken at well-defined normal working conditions. Using the baseline as reference, increases of power at any interval can be tracked by performing new measurements at similar working conditions. An increase of ~6-8 dB is considered enough to raise alarm and ~20 dB is regarded as serious.

Spectral trending involves trending the level of vibrations at all or a few select spectral lines (/frequencies). This works best for simple machines that have fewer significant spectral lines than complex machinery. Using to many spectral lines might cause data overload [13].

2.3.2.3 Windowing

When performing a frequency domain analysis, continuous signals need to be cropped into discrete segments of a limited time-interval. When cropping there is an issue with not knowing how the start and end of the signal continues outside of the selected interval. This issue might cause an offset to the entire signal. One way to surpass this is making the edges of the signal zero by multiplying the signal with a function that is zero at the ends and larger in the middle. This forces the analysis to ignore the edges and focus on the middle part. A function like this is called a window-function and the application of one such function on a signal is called windowing [18, pp. 36-37].

There are several different window-functions that amplify the middle section of the signal in different formations. One of the most common is called the Hanning window and can be used with stochastic signals. However, the Hanning window is not suitable when looking at transient events like shocks. For transient events a rectangular window should be used. A rectangular window does not affect the signal shape in a varying way like a Hanning window which is shaped like a haystack / a normal distribution curve. [18, pp. 36-37]

2.3.3 Time-frequency domain analysis

There is a third angle of vibration analysis called the time-frequency domain. The analysis methodology in the time-frequency domain is like the frequency-domain but the signal length is cropped down even further to investigate how the frequency content of the signal changes over time [10].

The time-frequency domain will not be investigated in this thesis.

2.4 Fault detection and diagnosis

2.4.1 Fault detection

The most basic method of monitoring vibrations is trending the overall vibration level over time. Often this is done using peak and/or RMS value with increasing values regarded as a sign of deteriorating conditions.

RMS is preferred over peak value due to the peak value's sensitivity to noise. Use of RMS is also the method described in SS-ISO 10816-3. However, as previously mentioned, overall vibrations do not provide information about the vibration source. Furthermore, to get a noticeable difference in RMS it may require significant increase of the overall vibration level, to the point that localized faults may have caused serious secondary damage and catastrophic failure [13, p. 61].

Waveform metrics like kurtosis is also used to detect faults in machine conditions. As kurtosis is a measure of the signal waveform, corresponding to the spikiness of the signal, an increasing value is regarded as sign of a worsening condition. The issue with using kurtosis for fault detection is the same reason as with RMS with the addition of the decreasing behaviour of kurtosis when a localized fault becomes distributed (described in 2.3.1.2). [13, p. 61]

Fault detection accuracy may improve by focusing the analysis to a narrower band of frequencies and using spectral comparison or spectral trending (described in 2.3.2.2) [13, p. 61].

2.4.2 Fault diagnosis

Fault diagnosis can be very difficult and to simplify the diagnostic process only frequencies that have significant changes in amplitude are analysed in detail. Distributed faults that cause an increase of the amplitude of some discrete frequencies, like unbalance or eccentricity, are easiest to diagnose. While localized faults like a cracked tooth is hard to diagnose and might only be detectable as a transient peak in the raw time domain signal [13, pp. 69-70].

2.4.3 Vibrations in different components

Different faults that may arise in machinery often generate vibrations with different spectral signatures. These signatures are often harmonics of the rotational speed, sidebands and/or high frequency noise. In terms of spectral analysis, the feature corresponding to the rotational speed of the component in question is referred to as first order (1x). Harmonic features corresponding to two times the rotational speed is referred to as second order (2x), and so on.

A guide to diagnosis of common faults using spectral features can be found in Appendix A.

2.4.3.1 Gears

Gears will normally generate peaks at both low and high frequencies (see Figure 4). First and second order rpm peaks will always be present in the spectral representation (e.g. DFT) of any gearbox. There will also be a peak at the Gear Mesh Frequency (GMF = number of teeth on gear x gear rpm). Also, there might be sidebands around the GMF spaced with the gear rpm. All these peaks are naturally occurring at low amplitudes but if the amplitude increases significantly alarm should be raised [5, pp. 115-116].

Distributed faults like eccentricity or gear misalignment will generally cause high amplitude harmonics or sidebands close to the GMF while localized faults like a cracked tooth will cause sidebands that are more widely spread across the spectrum [5, pp. 115-116].

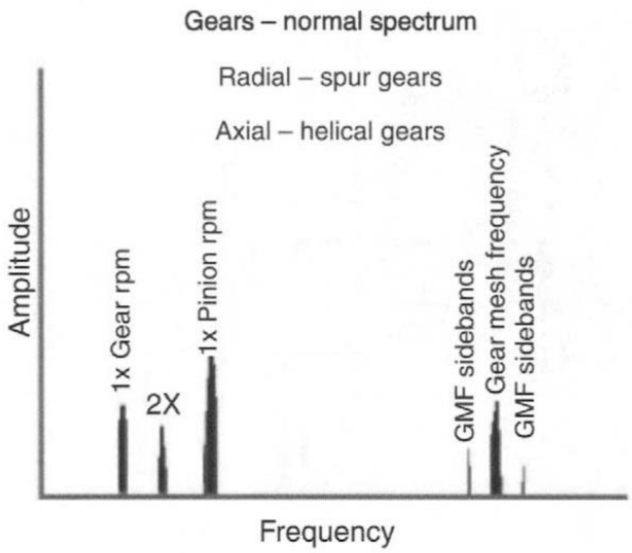

Figure 4. The normal spectrum of gears [5, p. 116]

2.4.3.2 Bearings

There are some fundamental bearing frequencies which will always be visible in the velocity spectrum possibly along with harmonics. These are the Ball Pass Frequency Inner (BPFI), Ball Pass Frequency Outer (BPFO), the Ball Pass Frequency (BPF) and the Fundamental Train Frequency (FTF) [19].

BPFI can be estimated as:0.6 x N x f, where N is the number of rolling elements and f is the rpm. BPFO can similarly be estimated as: 0.4 x N x f. BPF is estimated as: 0.2 x N x f and FTF as 0.4 x f.

In addition to the fundamental frequencies there are naturally occurring bearing resonances between 3-50 kHz. [19]

Bearing faults most often start showing as high frequency noise that will develop a noise-floor resembling a haystack in the spectrum. As the fault develops the noise-floor will widen and get higher in amplitude. There are 4 stages of bearing wear and the spectral properties of these are described in Appendix A table.

2.4.3.3 Axles

Like many other components, axles can be subject to for example looseness, misalignment or rotor rub. The spectral signatures associated with these issues can be found in Appendix A table 1.

When monitoring both the driving and the non-driving side of an axle the signal will most likely have the same signature and should in best case be the same amplitude. One might expect the driving side to have a slightly higher amplitude, as this side will to a larger extent be affected by adjacent components.

Determining alarm- and trip-levels for axles is best done by assuming a level based on prior measurements at a well-defined condition. If the current level turns out to be several times lower than the assumed alarm-level, then the level should be lowered. If it is not lowered, substantial increases in vibrations that might be critical, may go unnoticed.

3 Similar applications and implementation

3.1 Similar applications of vibration analysis

3.1.1 Stamping tools

To avoid expensive tool replacements, poor part quality, machine downtime and unscheduled maintenance, Ubhayaratne et al. suggest using audio signal analysis to evaluate tool wear that is not visible to the naked eye [20].

During trials a combination of procedures trimming, stamping and piercing was observed simultaneously throughout a series of 1500 parts. In order to analyse the different procedures separately a data extraction algorithm was developed. Vibration data was recorded and then analysed by evaluating the magnitude of the vibrations in the entire bandwidth and that of limited frequency bands. The analysis was done in both the time and the frequency domain also including an analysis of the RMS and peak-values of the signal.

In the study Ubhayaratne et al. [20] found that there was significant correlation between the recorded audio signal and tool wear. They could identify a specific frequency band that gave valuable information about the state of wear, making signs of wear detectable a significant amount of time before the wear has become severe and before failure. However, analysis of RMS and peak-value was found not to provide enough information to make conclusions of the tool wear [20].

3.1.2 Car body assembly Volvo Torslanda

At Volvo cars plant in Torslanda the company SPM Instrument AB has successfully implemented condition monitoring of two bolting stations used for assembling the car body to car platform [21].

A combination of vibration-monitoring using accelerometers and the shock pulse method (SPM) is used to determine the lubrication and mechanical condition of two axial bearings with adjoined ball screws on each bolting station. The measurements are performed continuously and when reaching unacceptable levels an alarm is issued directly to the equipment PLC. Each operation takes about 4 seconds, putting the measuring equipment under great strain.

In early January of 2019 the monitoring solution enabled the maintenance department to pre-schedule the change of a close to failure ball screw during scheduled downtime. An operation that usually takes 7 hours and could affect productivity [21].

3.1.3 Driveline Volvo CE

In the driveline of heavy construction equipment such as those manufactured by Volvo CE, there are many crucial components. The driveline enables torque to be transferred from the engine to the wheels via components like a torque converter, gearbox, clutches, bearings and axles. If any of these components fail it will render the equipment non-operational with costly downtimes as a result. When there is a failure the on-board diagnostic system will generate one or several failure codes based on simple rules and decision maps. This simplistic diagnostic tool is often not enough to find the root-cause of the problem and substantial manual inspection is needed as well, requiring skilled technicians and engineers [9].

To reduce unnecessary downtimes and facilitate easy and preventative maintenance, a methodology for using primarily vibration signals to monitor the health of the different components has been developed by Elisabeth Källström of Luleå University of Technology [9].

3.1.4 Cold roll press for aluminium

Dai et al. [14] has researched the use of vibration and sound emission monitoring of a cold roll press for aluminum. The objective was to achieve fault detection and diagnosis while using less measuring equipment and less time for measuring and data analysis. Dai et al. used a combination of sound intensity, statistical measures and FFT to determine the source of vibrations and the nature of damage. The ability to monitor the development of damage in complex machinery the authors say might help increase machine utilization rates and product output quality [14].

3.1.5 Paper industry

Two of the largest pulp mills in the world, Södra cell Värö, Sweden and Södra cell Mönsterås, Sweden has chosen to use vibrations for online monitoring of the mechanical condition of some crucial equipment. As part of a large investment in industry 4.0 the wire, press and dryer section at the plant in Värö and the woodchipper at the plant in Mönsterås have/will be fitted with several accelerometers that measure vibrations. The collected data is then digitally analysed in an online system that alerts operators and maintenance personnel when readings are high. The main objective of the investment is maximizing equipment availability [22] [23].

3.2 Implementation using machine learning

3.2.1 Basics of machine learning

Human brains can analyse and find patterns in data and use it to make qualified decisions but when the amount of data reaches a certain level the human brain cannot effectively comprehend all that data. What machine learning does is learn computers to draw conclusions similarly to a human by using historical data to train algorithms. A computer can store and analyse a higher volume of data in a much shorter time than any human [24].

The workflow of developing a predictive maintenance model using machine learning is can be summarized in 5 steps:

1. Data acquisition: The initial step is acquiring the necessary data. The model input and output and may come from many different sources in and around the modelled equipment.
2. Pre-processing of data: The acquired data then needs to be pre-processed to remove noise, handle outliers and to combine data from different sources.

3. Feature extraction: Instead of running an entire set of features and extreme amounts of data through the machine learning model, feature extraction is applied to identify features that carry a high level of information. This way high-dimensional problems can be reduced to a few features that carry most of the information needed to understand the predictive model.
4. Training: The model can be trained using either supervised or unsupervised learning. Using supervised learning means telling the model if the data is good/bad, setting thresholds for different conditions, and/or giving the model estimations of the equipment's actual remaining useful life. Unsupervised learning means the model itself finds hidden patterns or intrinsic structures in data that is later classified using different classification methods.
5. Deployment: The final step is to let the model start working by deploying it to the platform where it will be used [25] [24].

3.2.1.1 Feature extraction

Features are also called condition indicators and can be described as alternative ways to observe data to easier differentiate good and bad conditions and sources of vibrations. To further understand the concept; imagine a cone and a cylinder, while both look like circles when observed from the top, there is a difference between the two when looking at them from the side that allows us to draw the conclusion that one is a cone and the other a cylinder.

When observing data in the time-domain it can all seem a bit messy and data seems similar but when using different condition indicators to look at it, information may become clearer. In machine learning different features can simultaneously be used to train the model which may be beneficial when differentiating different fault types or conditions [26].

There are different condition indicators that can be used depending on if the data is viewed from the time-/frequency/time-frequency domain. Examples of different features used in different domains can be found in Table 2 below. [26]

Table 2. Condition indicators used in different domains [26]

Time domain	Frequency domain	Time-frequency domain
- Mean - Standard deviation - Skewness - Root-mean-square (RMS) - Kurtosis - **…**	- Power bandwidth - Mean frequency - Peak values - Peak frequencies - Harmonies - …	- Spectral entropy - Spectral kurtosis - …

3.2.1.2 Supervised and unsupervised learning

Supervised learning trains the model by supplying it with historical input and labelled output data. With supervised learning the model is told what the output or the label of the data is for a certain input and the algorithm learns by comparing the input to the actual output.

There are two main paths to supervised learning: regression and classification [24].

If the output is not known, then unsupervised learning can be used. Unsupervised learning is used to find patterns within un-labelled data and to make clusters of data with similar patterns.

Clustering is the main method used to classify data when using unsupervised learning [24].

3.3 Similar applications of vibration analysis with machine learning

3.3.1 Cutting tools

In metal cutting processes the specific cutting energy will affect not only the surface integrity but also the process sustainability. The present way of measuring the specific cutting energy is limited and complex. Ziye Liu and Yuebin Guo [27] suggest using a combined approach of machine learning and process mechanics to predict the specific cutting energy in milling. This data driven machine learning approach proved to predict the specific cutting energy better than the traditional mechanics models [27].

3.3.2 Gas and Oil Extraction Equipment

The international oil field service company Baker Hughes has several extraction sites where oil is tapped around the clock. On the sites, large trucks equipped with pumps are used to tap the oil wells. At times as many as 20 trucks are pumping oil simultaneously [28].

Within the pumps are valves, seals, plunges and more that may cause damages beyond repair if worn to the point of failure. To prevent costly failures and inactive wells, Baker Hughes can have spare trucks on site or perform preventative maintenance. In attempt to bypass these options, engineers at Baker Hughes has used Matlab and data analytics to develop predictive maintenance software for monitoring pump health. They used several sensors to monitor different parameters and could later determine that the most important condition indicators for health monitoring of pumps are pressure, vibration, and timing. The data was used to create and train a data driven model that was later validated using data collected after the model was built [28].

4 Data analysis

The analysis will be segmented based on the analysed component and on which press this component is situated. Any similarities between the corresponding components on the different presses will be discussed as it appears. So will any assumptions about the measurement's conditions and any diagnostics.

The ISO 10816-3 guideline RMS-limit of 4,5 mm/s will be used continuously as a reference limit for all components even though this limit is applicable only to motors.

All code used for analysis can be found in Appendix A.

4.1 Sensor placement

The placement of the accelerometers in this thesis is as stated in Table 3 below. In Figure 5 the placement of each sensor 1-10 can be seen on the schematic overview of a basic mechanical press.

Table 3. Placement of sensors.

SENSOR	PLACEMENT
1	Motor axle, driving side (front)
2	Motor axle, non-driving side (back)
3	Pulley wheel, side facing away from motor (front)
4	Pulley wheel, side facing motor (back)
5	Gearbox axle in (front)
6	Gearbox axle in (back)
7	Secondary axle, side by eccentric wheel (left crank) (front)
8	Secondary axle, side by gearbox (left crank) (back)
9	Secondary axle, side by eccentric wheel (right crank) (front)
10	Secondary axle, side by gearbox (right crank) (back)

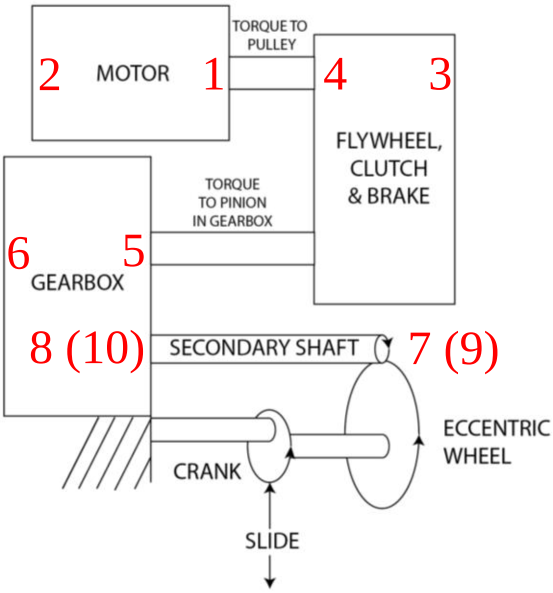

Figure 5. Placement of sensors 1-10 on a schematic overview of the press.

4.2 Vibration analysis in Matlab

To reach a conclusion whether vibration analysis is a helpful tool for predictive maintenance on a mechanical press, data must be analysed to find reoccurring patterns and increasing trends in the frequency and amplitude of vibrations. In this thesis Matlab will be used to make such analysis. The work done in Matlab will follow the structure of the 4 latter steps in Figure 2; frequency analysis (digital filtering, Fast Fourier Transform), measurement data processing and graphing. The methodology is further explained in 4.2.1.

A combination of power spectral density (PSD), fast Fourier transform (FFT) and the statistical measures RMS and kurtosis are used for this analysis.

PSD is chosen as it is a useable tool for trending the distribution of vibrations in different bandwidths and is therefore good for spectral trending and comparison. FFT is used as it is the quickest way to separate the frequencies of the signal which may help with diagnosis. RMS and kurtosis are both traditional and basic ways of condition monitoring and as these require little computer power, they are interesting from an implementation point-of-view as well. Furthermore, RMS is the ISO-recommended condition monitoring measure for motors etc.

Components are separated into two cases depending on if their real condition is known or not. The cases are described as following:

1. Conditions corresponding to previously recorded data is known and/or different conditions of the components has been captured
2. Condition is not known and/or has not changed.

If the case is number 1 then the data is labelled with conditions (output) 'good', 'decent' or 'bad' and both the PSD and the DFT along with statistical measures for data of different conditions are manually compared to find certain features or patterns that characterize different conditions and that could be used for spectral comparison and/or -trending. This should make it possible to differentiate between conditions in new data based on how well the new data matches features and patterns of old data. Meaning it should also be possible to use classification and machine learning.

However, if the case is instead case number 2, sorting based on patterns and peaks is more difficult. In this case the output is initially assumed to be constantly 'decent' and the PSD along with statistical measures are analysed and compared manually to see if there is data that shows peculiar behaviour, for example if there are clusters of peaks that deviate from the normal pattern, or if there is an increasing trend in PSD level or RMS. The assumed condition may be changed based on the findings to see if differences resound in all 4 analysis measures.

4.2.1 Analysis methodology

An overview of the analysis methodology can be found in Figure 6 below.

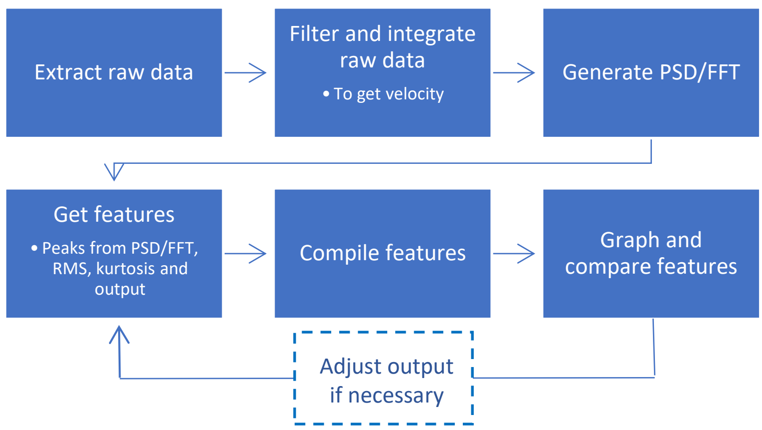

Figure 6. Flowchart of the general analysis methodology.

4.2.1.1 Feature extraction

Measurements from the front sensor (driving side) of the motor on press 2 will be used as an example of how feature extraction and analysis is done in this thesis. This component has no known/no change of condition (output) and is therefore classified as case 2.

Features are extracted only from the velocity PSD/FFT and not the acceleration PSD/FFT. This is done based on the assumption that the frequencies of most interest are within the range of 10-1000 Hz and velocity is therefore preferable due to reasons discussed in 2.3.1. The reason frequencies are assumeably within this *interval is the size of the components is question. As these are large in mass, they will have a large moment of inertia and are therefore more suseptable to low frequency vibrations. However, with components like bearings, high frequencies are of great interest for fault detection which should be included in future implementations but is excluded in this thesis.*

Furthermore RMS is calculated in the interval of 20-2000Hz besause of the previously stated reasons.

The data used in the Matlab analysis is extracted from the software which is currently being used for this application at Volvo. The segment of the signal being used is either from idle operation when the slide is at the top, the clutch is not engaged and the motor/pulley rotates freely (for sensors on motor and pulley), or tool down when the clutch is engaged and the slide goes down (for all other sensors).

After importing the raw acceleration data, the first step of the Matlab analysis is filtering, integrating the acceleration to velocity and filtering again to get the filtered velocity. The filtered velocity is then used to generate the power spectrum density (PSD). The time domain velocity signal can be seen in the top figure of Figure 7 and the PSD in the lower figure. The blue signal is unfiltered velocity and the red is the filtered velocity.

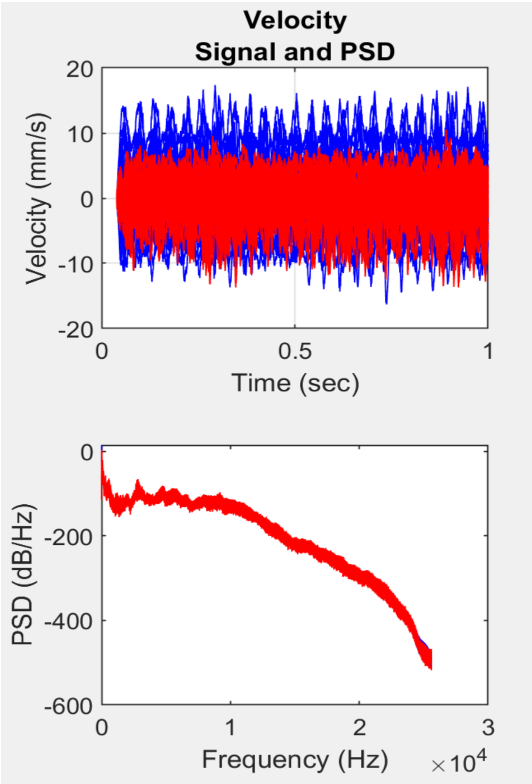

Figure 7. Time domain signal (top) and power spectrum denisty (bottom) of unfiltered (blue) and filtered (red) velocity. Both figures show the signal from the front (driving side) sensor on the motor of press 2.

Note that a segment at the beginning of the velocity signal has been cropped out and is not used (see top Figure 7). This has been done due to some transient behaviour. Possible causes and solutions to this issue will be discussed further in section 0.

Discussion.

The first 25 peaks of the velocity PSD is extracted into an array of the corrensponding amplitudes and frequencies of the peaks (see Figure 8. The red is the PSD of all measurements and the black is circles around the first 25 peaks of each measurement). The statistical time domain measurements (velocity RMS and kurtosis) are compiled together with the previously extracted peaks and every measurement's corresponding output, to form a large table of features. The velocity RMS has been calculated from the FFT using Eq. 1 and the frequency-limits $f_1 \approx 20$ Hz and $f_2 \approx 2000$ Hz. Kurtosis is calculated from the filtered velocity.

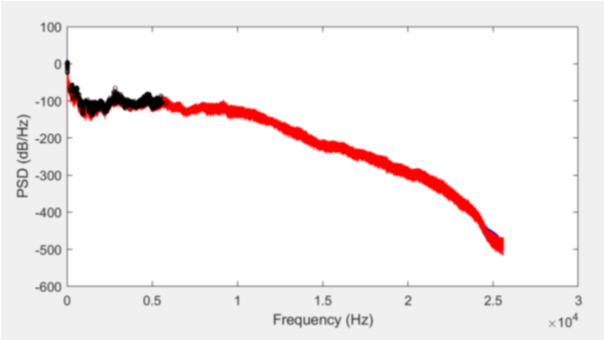

Figure 8. Identification of the first 25 peaks in the filtered velocity PSD. Red is PSD of all measurements, black is circles around the first 25 peaks of each measurement. The signal is from the front (driving side) sensor on the motor of press 2.

The same procedure is repeated for the DFT of the signal using FFT with a Hanning window and extracting the first 25 peaks in the spectrum as features for each measurement.

All of the features (RMS, kurtosis, peaks from FFT and PSD) will be investigated to find if they can be used to represent the condition of the press and if so, which ones best represent the condition.

4.2.1.2 Feature analysis

This component has no known/no change of condition (output) and all measurements are therefore initially assumed 'decent'.

Initially the previously extracted PSD peaks are investigated. This is to identify any clear differences or increasing levels that may indicate separate conditions. All measurements are plotted in the same window (see Figure 9 below).

Judging from the resulting PSD-peaks there are no clear differences to be found between measurements. The peaks at each frequency seem to lie within a span of about ±10-15 dB which exceeds the increase of ~6 dB that is recommended to cause alarm and the level of some measurements does differ a bit more around 1500 Hz and there some higher peaks at 3000 Hz but there are no clear outliers in the data. If there was several different conditions it would be easier to compare the levels, especially if there was measurements from a clearly defined 'normal' condition that could be regarded as a base level for spectral comparison.

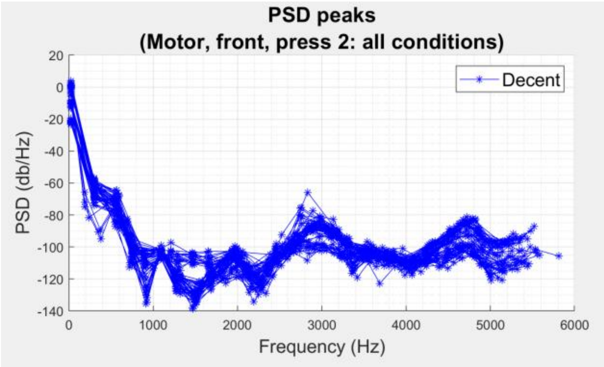

Figure 9. Distribution of PSD peaks for different conditions. All measurements are from the front sensor on the motor of press 2.

Also looking at the FFT peaks in Figure 10 below, it is difficult to draw any conclusions about the condition or diagnosis of the motor. There are rather high amplitudes at 25 Hz and also at 50 and 75 Hz (assumed corresponding to 1x, 2x and 3x as the motor rpm is 1350rpm/22.5 Hz according to the rating plate but might differ a bit from real life), but it is hard to tell how serious these levels are as there is nothing to compare to.

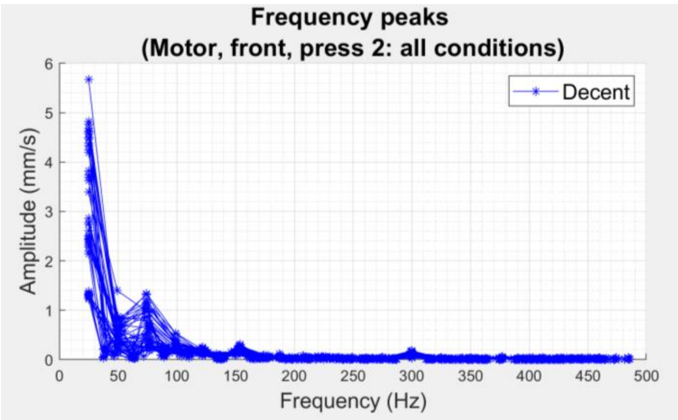

Figure 10. Distribution of FFT peaks. All measurements are from the front sensor on the motor of press 2.

When looking at the statistical features RMS of velocity and kurtosis (Figure 11 below), there are clearly some variation. The dotted line in the upper figure of Figure 11 is the ISO 10816-3 guideline limit of 4,5mm/s between zone C (levels of vibrations considered unacceptable for long-term operation) and zone D (levels of vibrations considered harmful to the health of the machinery). Measurements 30-44 and measurement 16 are all above this limit. Measurements 30-44 have high RMS, indicating that the overall vibration-level is dangerously high. It is not really possible to read out any information about the condition from the kurtosis.

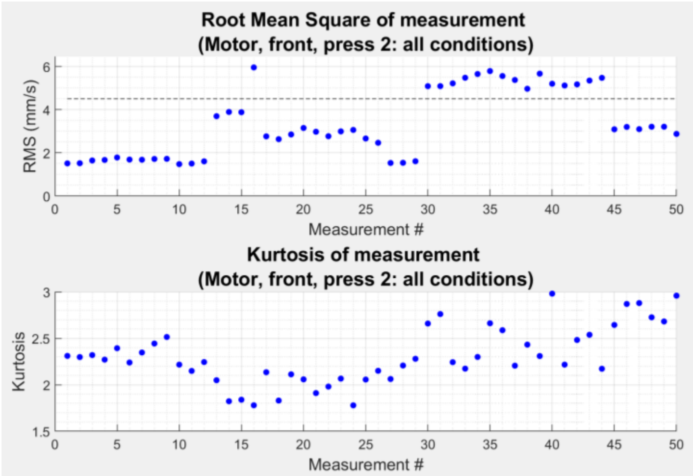

Figure 11. Statistical features for each measurement of the front sensor on the motor of press 2. Upper figure: RMS of velocity. Dashed line in figure is the ISO-limit 4,5 mm/s. Lower figure: Kurtosis.

New conditions are assigned the different measurements to investigate any patterns of PSD and FFT that are recurring for different levels of RMS. All measurements above the dotted line are changed to 'bad', measurements 13-15 and 17-26 changed to 'decent' and the rest to 'good' (for reference see Figure 14). The result of PSD and FFT can be seen in Figure 12 and Figure 13.

Regarding the PSD in Figure 12 below there are some things that seem reoccuring for 'bad' conditions. For example the level at ~1500 Hz is higher than that of 'decent' and 'good' condition. However, the PSD pattern of 'decent' and 'good' are quite similar.

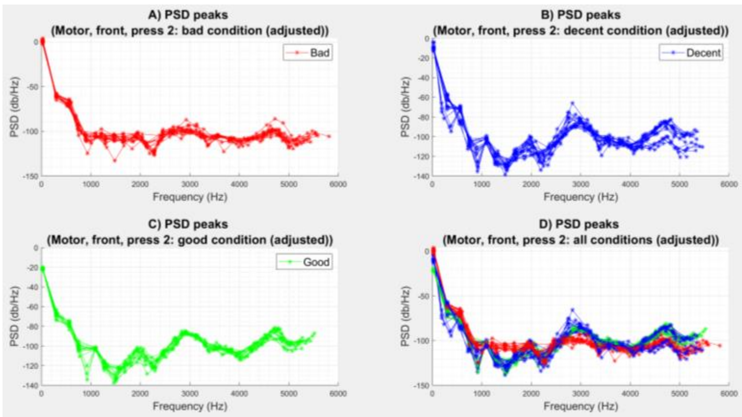

Figure 12. Distribution of PSD peaks with adjusted output. All measurements are from the front sensor on the motor of press 2.

Looking at the FFT in Figure 13 below, we see that for ‘good’ condition the 1x peak at ~25 Hz is much lower than the 1x peak for ‘decent’ condition. So the RMS level seems to be somewhat reliable for condition monitoring of motors. Confirming the method recommended in ISO 10816-3, although the appropriate ALARM-level of this component is not known nor is it certain that these assumed conclusions are correct as the actual condition is not known.

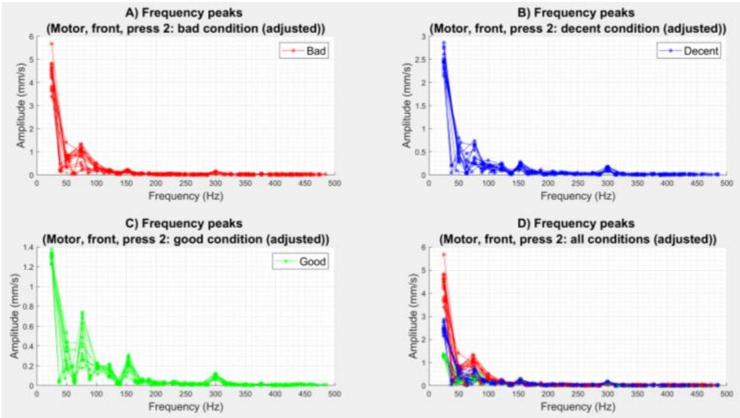

Figure 13. Distribution of FFT peaks with adjusted output. All measurements are from the front sensor on the motor of press 2.

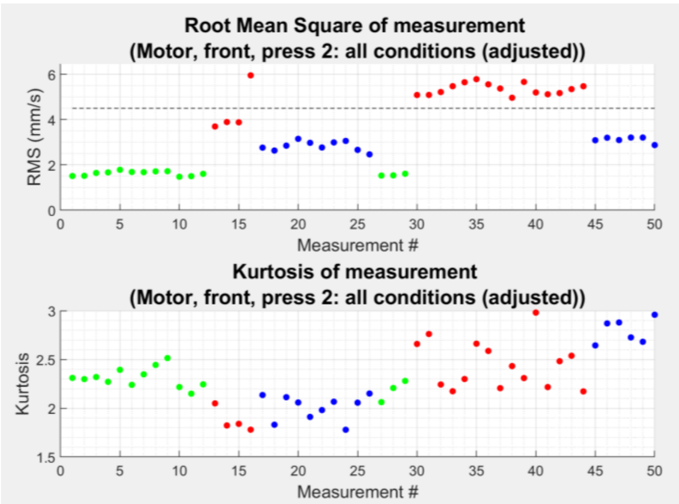

Figure 14. Statistical features with adjusted output for each measurement of the front sensor on the motor of press 2. Upper figure: RMS of velocity. Dashed line in figure is the ISO-limit 4,5 mm/s. Lower figure: Kurtosis.

4.3 Motor

4.3.1 Front sensor

4.3.1.1 Press 2

See 4.2.1.2 *Feature analysis*.

4.3.1.2 Press 4

This component has no known/no change of condition (output) and all measurements are therefore initially assumed 'decent'.

The pattern of PSD and FFT at the front of the motor of press 4 (seen in Figure 15 and Figure 16 below) is more consistent and the peaks are generally lower in amplitude than at the front of the motor on press 2. One difference that should be noticed is the pattern of peaks at ~41- 42 Hz in the FFT (Figure 16 below). This is at approximately 1.5x and might indicate slight internal assembly looseness or rotor rub.

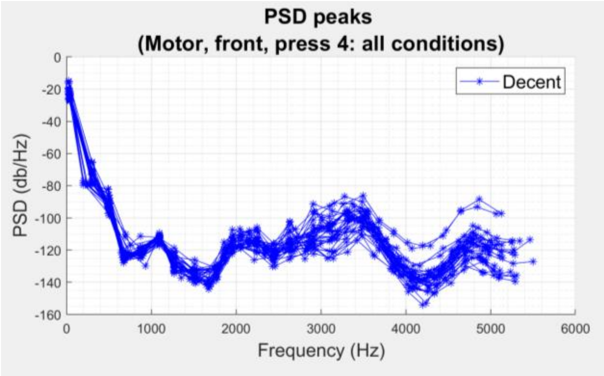

Figure 15. Distribution of PSD peaks. All measurements are from the front sensor on the motor of press 4.

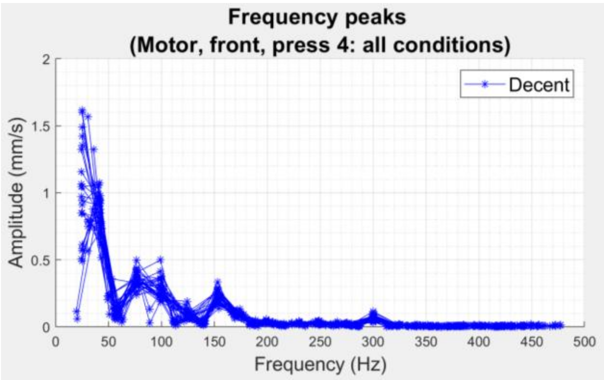

Figure 16. Distribution of FFT peaks. All measurements are from the front sensor on the motor of press 4.

RMS amplitude at the front end of the motor on press 4 is significantly more consistent than that on press 2 but the kurtosis is irregular. It is at a level that is assumed indicatory of 'good'/'decent' condition (compare Figure 14 above and Figure 17 below).

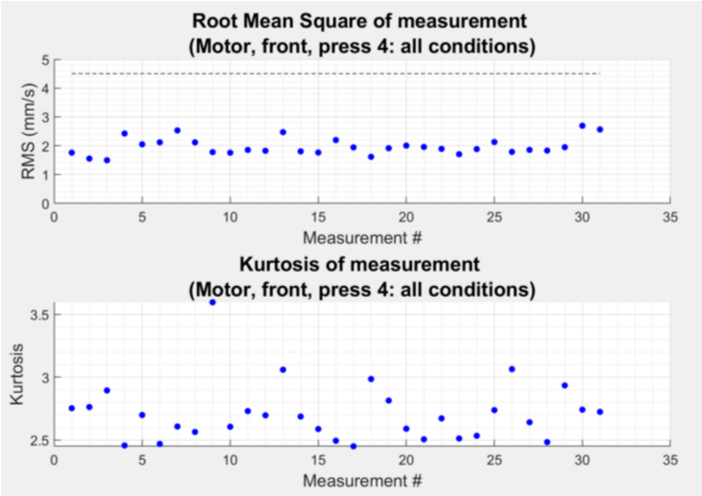

Figure 17. Statistical features for each measurement of the front sensor on the motor of press 4. Upper figure: RMS of velocity. Dashed line in figure is the ISO-limit 4,5 mm/s. Lower figure: Kurtosis.

4.3.2 Back sensor

4.3.2.1 Press 2

This component has no known/no change of condition (output) and all measurements are therefore initially assumed 'decent'.

Compared to the front sensor on the motor of press 2, the general PSD-level is lower at the back (compare Figure 9 above and
Figure 18 below). This is not unexpected as the front side is the driving side and will be affected by vibrations of the connected components (pulley) to a greater extent.

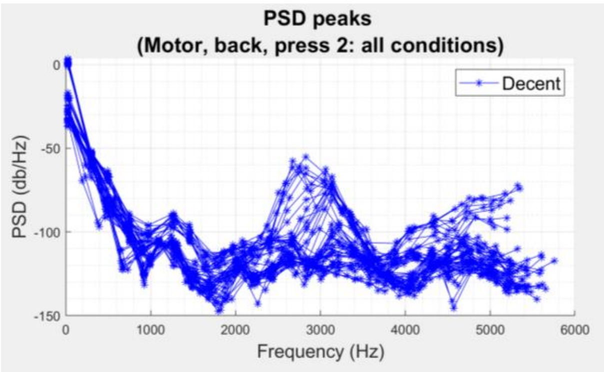

Figure 18. Distribution of PSD peaks. All measurements are from the back sensor on the motor of press 2.

Regarding the FFT, peaks are like the peaks at the front and correspond to 1x, 2x and so on (see Figure 19 below).

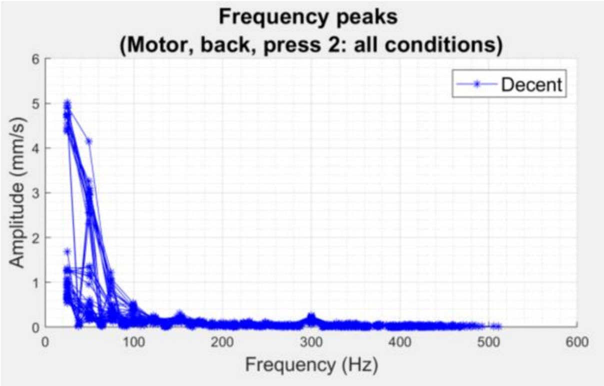

Figure 19. Distribution of FFT peaks. All measurements are from the back sensor on the motor of press 2.

Regarding RMS and kurtosis; RMS is once again high for measurements 30-44 (taken at the same time as measurements 30-44 at the front), indicating that any present fault is not only localized to the front of the motor. Kurtosis does not seem to provide any straightforward information. Once again, the measurements above the 4,5 mm/s RMS limit are assigned the condition 'bad' and the other measurements are classified accordingly (see Figure 20 and adjusted result in Figure 23 below).

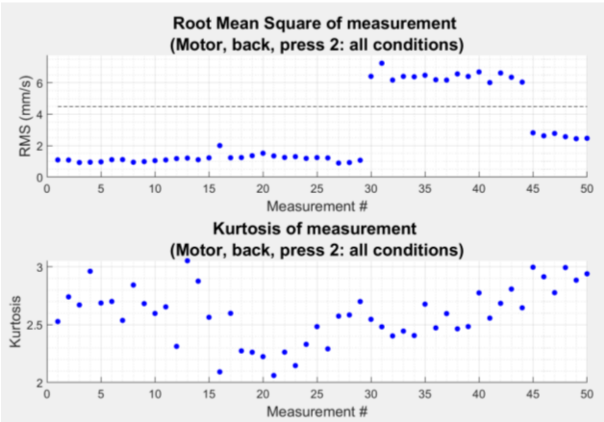

Figure 20. Statistical features for each measurement of the back sensor on the motor of press 2. Upper figure: RMS of velocity. Dashed line in figure is the ISO-limit 4,5 mm/s. Lower figure: Kurtosis.

Like with the adjusted output of the measurements from the front side of the sensor, the pattern of PSD and FFT for different conditions in Figure 21 and Figure 22 below, seem to match well and once again the amplitude of the FFT 1x peak is the main difference between ‘good’ and ‘bad’.

The high PSD around ~3000 Hz is caused to some haystack-behaviour around this frequency. What is causing this is unknown but might be indicating a bad condition bearing.

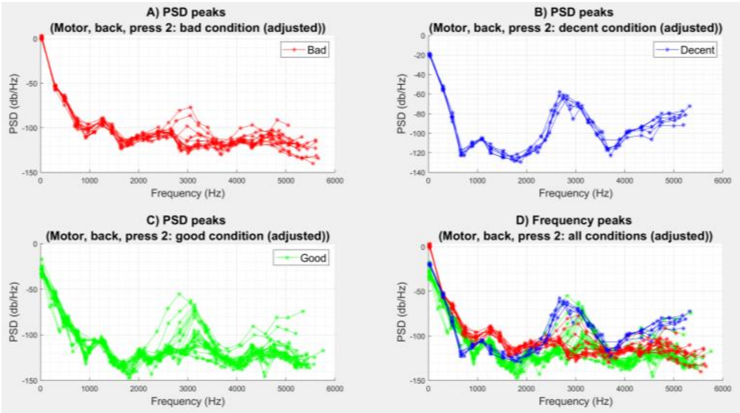

Figure 21. Distribution of PSD peaks with adjusted output. All measurements are from the back sensor on the motor of press 2.

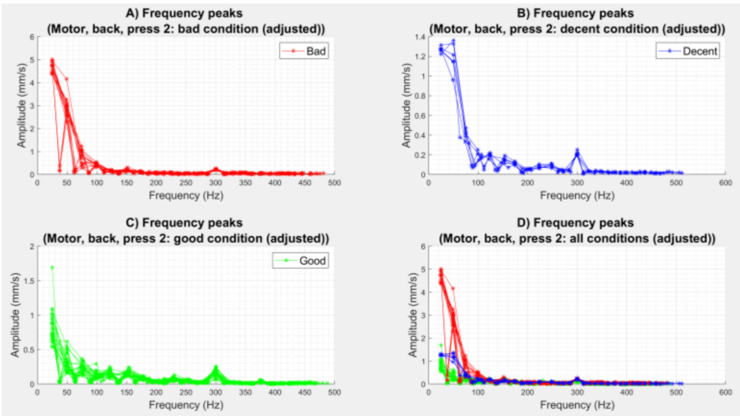

Figure 22. Distribution of FFT peaks with adjusted output. All measurements are from the back sensor on the motor of press 2.

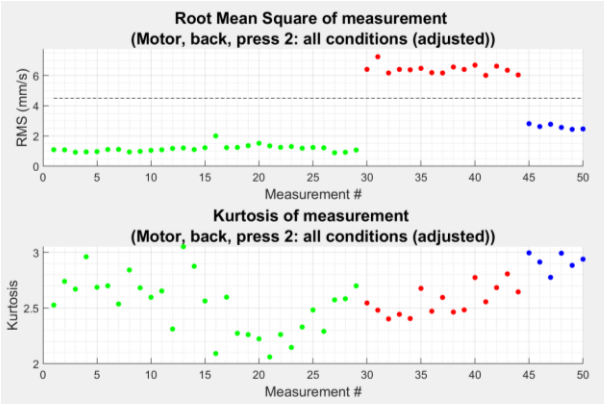

Figure 23. Statistical features with adjusted output for each measurement of the back sensor on the motor of press 4. Upper figure: RMS of velocity. Dashed line in figure is the ISO-limit 4,5 mm/s. Lower figure: Kurtosis.

4.3.2.2 Press 4

This component has no known/no change of condition (output) and all measurements are therefore initially assumed 'decent'.

Similar conclusions to the front sensor measurements of the the motor of press 4. Once again the measurements at the back (Figure 24, Figure 25 and Figure 26 below) are smaller than at the front which is the driving side (see Figure 15, Figure 16 and Figure 17 above), which is expected.

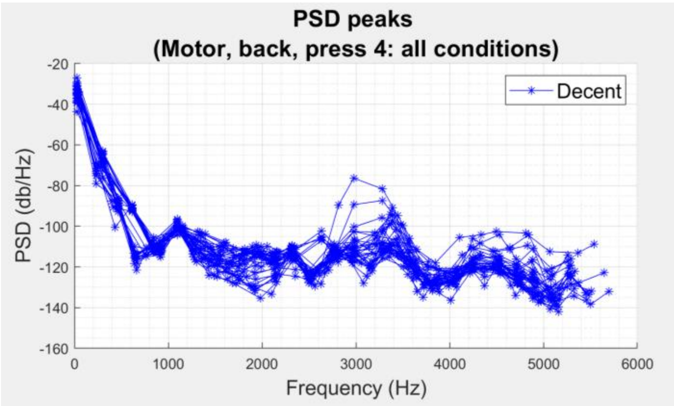

Figure 24. Distribution of PSD peaks. All measurements are from the back sensor on the motor of press 4.

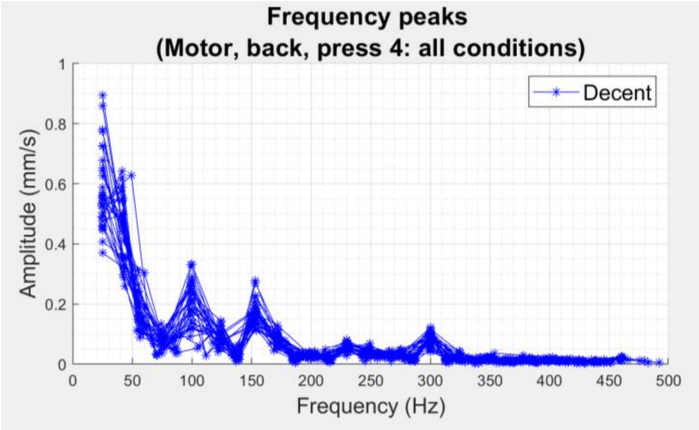

Figure 25. Distribution of FFT peaks. All measurements are from the back sensor on the motor of press 4.

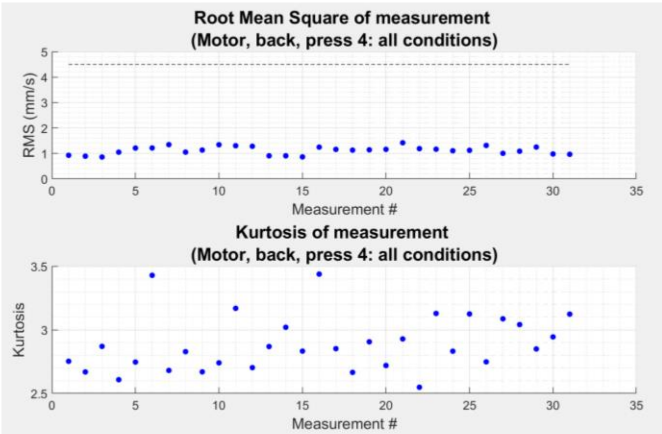

Figure 26. Statistical features for each measurement of the back sensor on the motor of press 4. Upper figure: RMS of velocity. Dashed line in figure is the ISO-limit 4,5 mm/s. Lower figure: Kurtosis.

4.4 Pulley

4.4.1 Front sensor

4.4.1.1 Press 2

The front sensor measurements of this component have known/different conditions (outputs) and all measurements are therefore initially labelled accordingly.

This is one of the components with the most recorded conditions. It is assumed that the condition of the pulley is ‘decent’ during the period prior to refurbishment of the press performed during summer 2018. Furthermore, the condition is assumed as ‘bad’ for measurements 30-44 that are taken just before the pulley breaks down due to bearing-failure. All measurements after this are assumed to be of a ‘good’ condition. Which bearing (front or back) that was the reason of failure has not been confirmed.

It is possible to tell the difference between different conditions by looking at the PSD in Figure 27 below. ‘Good’ condition is easiest recognizable by a lower level at around 2500 Hz. It is more difficult to distinguish ‘bad’ from ‘decent’, but it seems that a ‘bad’ condition will generally have a higher level of PSD at 600-800 Hz and at ~1400 Hz.

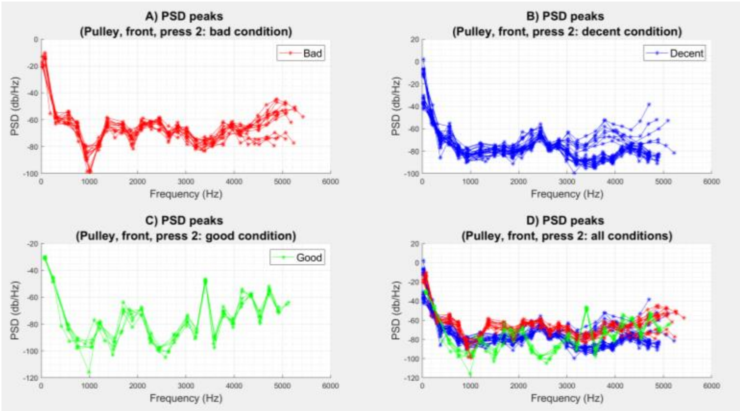

Figure 27. Distribution of PSD peaks for different conditions. All measurements are from the front sensor on the pulley of press 2.

Looking at the distribution of FFT peaks in Figure 28 below it is quite easy to deduct some characteristic behaviours associated to the conditions ‘bad’ and ‘decent’ respectively. Peaks at ~25Hz are recurring for both conditions, which is unsurprising as this is corresponding to the motor’s rotational velocity of 1350 rpm which is presumably driving the pulley at the same speed. However, the amplitude at ~25Hz is generally higher for the ‘decent’ condition than the ‘bad’ (compare Figure 28 D).

Looking at the 2x and 3x peaks at ~50Hz and ~75Hz, the amplitude is significantly higher for the ‘bad’ condition, especially the 3x peak. There is also an occurrence of peaks at ~37,5Hz and ~62,5Hz which is the order 1,5x and 2,5x. Although these peaks are mostly noticeable in ‘good’ condition and have a relatively low amplitude, they may be indications of misalignment or looseness.

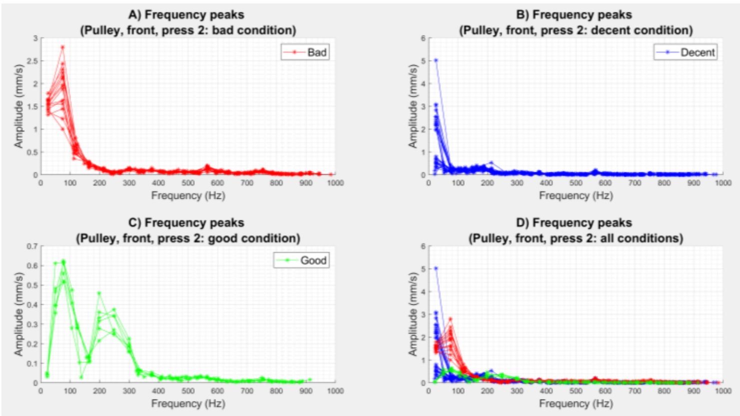

Figure 28. Distribution of FFT peaks for different conditions. All measurements are from the front sensor on the pulley of press 2.

Looking at RMS (upper graph in Figure 29 below) it is seen that the assumed conditions do not correspond well with the amplitude of RMS. The RMS of peak 13 to 26, which are assumed as ‘decent’ condition are at the same level or above that of peak 30 to 44 which are assumed ‘bad’, also noting that the only measurement with RMS above the ISO-recommended level of 4,5 mm/s is in this interval. Although noting that the 4,5 mm/s guideline is not necesserily applicable on this specific component nor pulleys in general. Furthermore, peak 1-12 and 27-29 which are assumed ‘decent’ are on a level below peak 45 to 50 which are ‘good’. This is also reflected in Figure 28 D) above where we see that the peaks of some of the ‘decent’ measurements are very similar in amplitude to the ‘good’ measurements, especially with regards to amplitude of the peak at ~25Hz which is uncharacteristically low. If the assumed condition of measurements 1-12 and 27-29 is changed from ‘decent’ to ‘good’, the distribution of peaks and statistical measurements instead look like in Figure 31 and Figure 32 below.

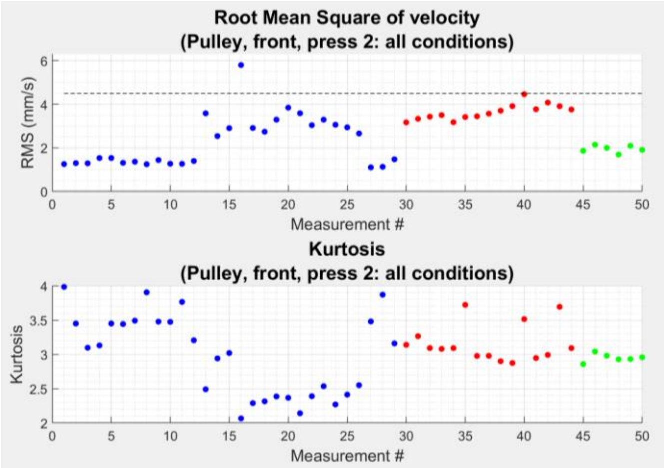

Figure 29. Statistical features for each measurement of the front sensor on the pulley of press 2. Upper figure: RMS of velocity. Dashed line in figure is the ISO-limit 4,5 mm/s. Middle figure: Kurtosis. Lower figure: Mean absolute acceleration.

With the adjusted output the distribution of FFT peaks seems to make more sense. The amplitude and pattern of measurements changed from ‘decent’ to ‘good’ appear to match well with the measurements initially assumed ‘good’. This is also an indication that RMS works well to tell whether a measurement is good but it not enough to differentiate between ‘decent’ and ‘bad’ as this requires further investigation of for example FFT peaks. With that said, the adjusted condition does not match up well with the other peaks when looking at PSD in Figure 30 but either way the ‘bad’ condition is distinguishable. Regarding kurtosis, the level does not provide any definite conclusions about the condition. It rather seems that kurtosis is contradictory at times. The guidelines previously discussed in 2.3.1.2 that specify kurtosis above 4 is sign of bad conditions is not applicable either.

If the bearing is a rolling element bearing it is possible to investigate to amplitude of the BPFI and BPFO (ball pass frequency inner/-outer) by FFT. An increase of these levels is indicative that failure is near. To do this it is necessary to know the number of rolling element and then the approximations BPFO ~0.4 x N x F and BPFI ~0.6 x N x F can be made. In this thesis these things are not known.

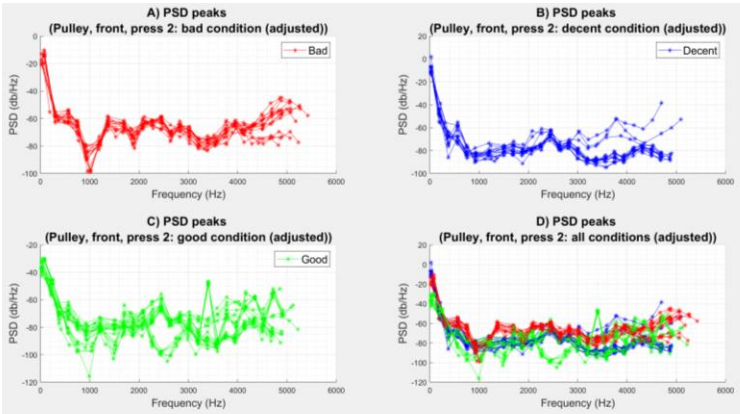

Figure 30. Distribution of PSD peaks with adjusted output for different conditions. All measurements are from the front sensor on the pulley of press 2.

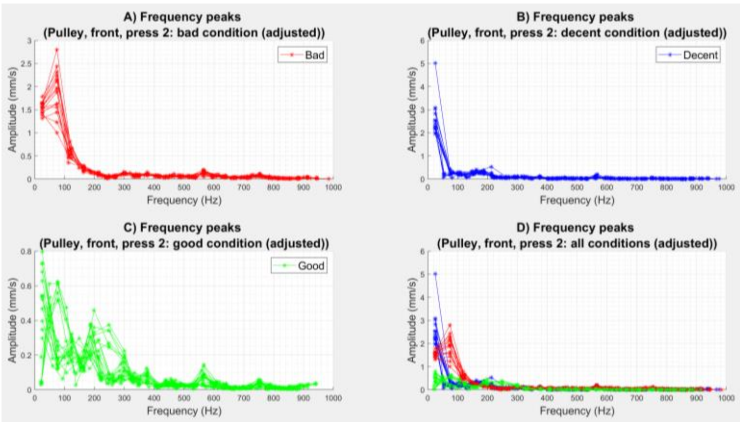

Figure 31. Distribution of FFT peaks with adjusted output for different conditions. All measurements are from the front sensor on the pulley of press 2.

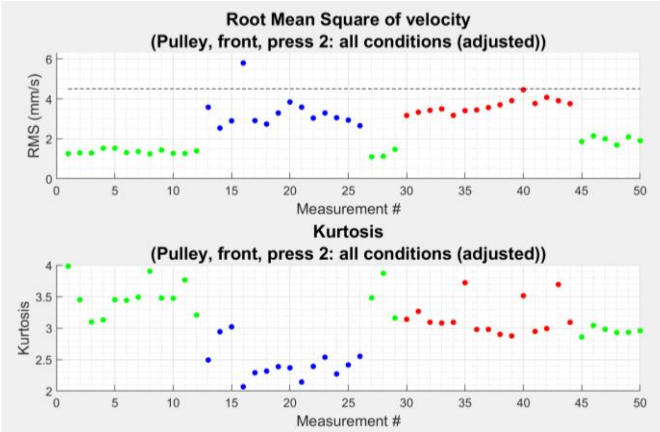

Figure 32. Statistical features with adjusted output for each measurement of the front sensor on the pulley of press 2. Upper figure: RMS of velocity. Dashed line in figure is the ISO-limit 4,5 mm/s. Lower figure: Kurtosis.

With bearings the high frequency noise-floor widens and increases in amplitude when failure is close. This behaviour can be confirmed by looking at the complete FFT of 'good' and 'bad' measurements (see Figure 33 below).

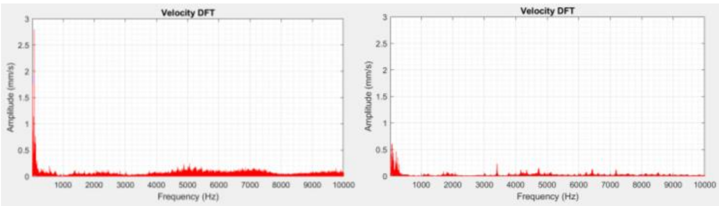

Figure 33. Comparison of noise-floor between 'bad' measurements 30-44 (left) and 'good' measurements 45-50 (right)

4.4.1.2 Press 4

This component has no known/no change of condition (output) and all measurements are therefore initially assumed 'decent'.

From the results in Figure 34, Figure 35 and Figure 36 below it is possible to make the conclusion that the condition of the pulley on press 4 is much more stable than that of the pulley on press 2. Judging by the amplitude of peaks from PSD/FFT and RMS, a 'decent' condition seems like a good assumption. Some irregularities are present like the splay of the peaks above ~2000 Hz in PSD. This may be due to outside noise. Also, the reason behind the irregular pattern of kurtosis is unclear.

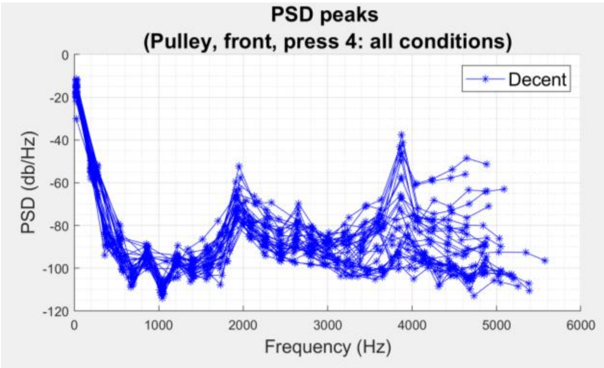

Figure 34. Distribution of PSD peaks. All measurements are from the front sensor on the pulley of press 4.

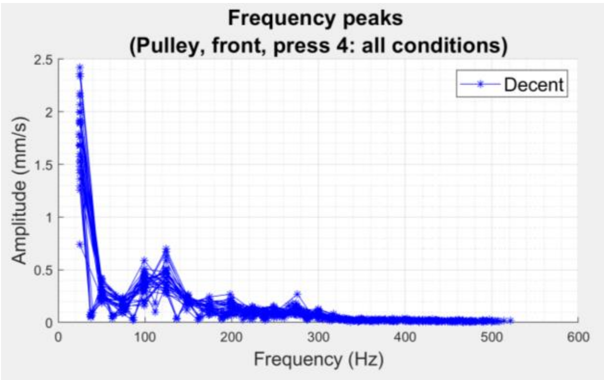

Figure 35. Distribution of FFT peaks. All measurements are from the front sensor on the pulley of press 4.

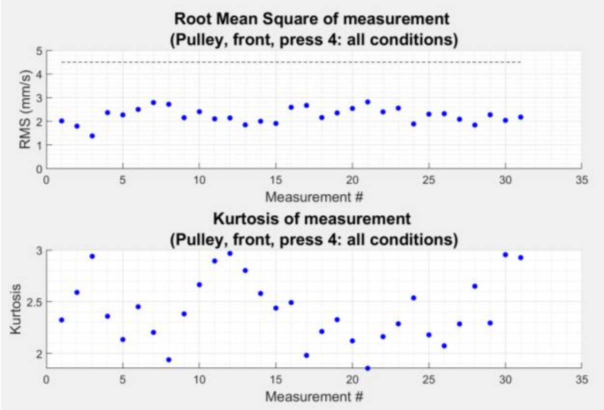

Figure 36. Statistical features for each measurement of the front sensor on the pulley of press 4. Upper figure: RMS of velocity. Dashed line in figure is the ISO-limit 4,5 mm/s. Lower figure: Kurtosis.

4.4.2 Back sensor

4.4.2.1 Press 2

The back sensor of this component has no known/no change of condition (output) and all measurements are therefore initially assumed 'decent'.

All measurements from the back sensor on the pulley of press 2 are taken prior to refurbishing in summer 2018, when the pulley condition was assumed 'decent'. However, with the adjusted conditions from the previous analysis of the front pulley measurements one can assume the same change of condition is noticeable by the back sensor too as the bearings on which the sensors measure is connected by the same axle. Noting that all 29 measurements at the back sensor are taken at the same time as the first 29 measurements at the front found in section 4.4.1.1.

With this adjustment the resulting distribution of PSD, FFT and statistical features can be seen in Figure 36, Figure 37 and Figure 38 respectively. The adjustment of conditions appears to correspond well to both the amplitude of FFT and the velocity RMS in the same way it did for the front sensor of the pulley.

There are no clear patterns in the PSD of this data (see Figure 36 below). Only major difference visible in Figure 37 is the level around 25 Hz.

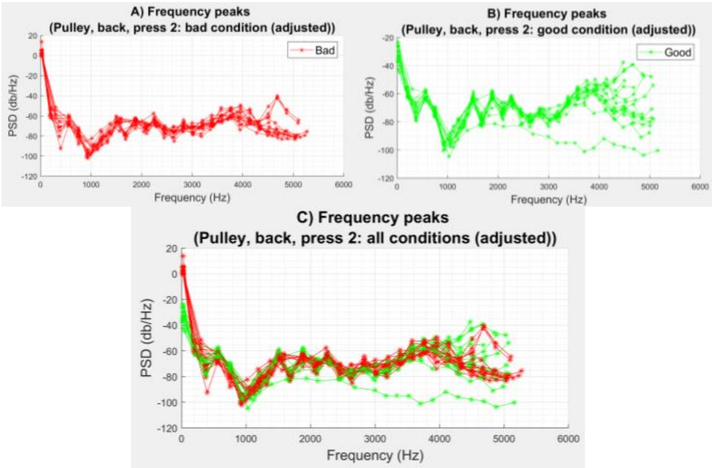

Figure 37. Distribution of FFT peaks with adjusted output for different conditions. All measurements are from the back sensor on the pulley of press 2.

With the FFT (see Figure 37 below), peaks are prevalent at 25 Hz and the amplitude of the ‘bad’ measurements are much higher than the ‘good’ at this frequency.

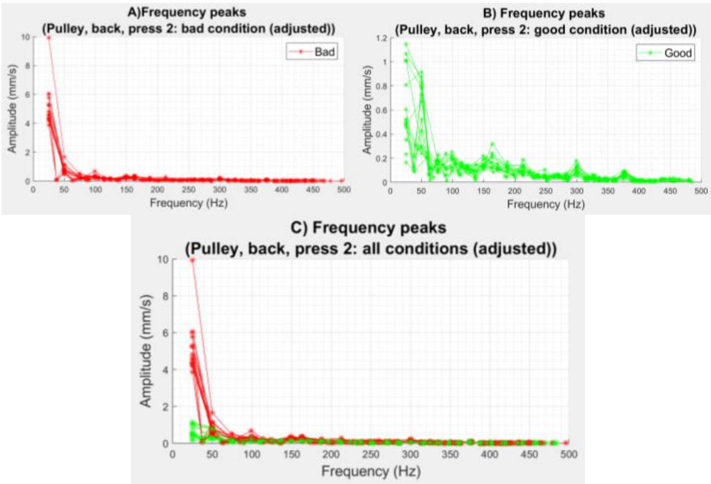

Figure 38. Distribution of FFT peaks with adjusted output for different conditions. All measurements are from the back sensor on the pulley of press 2.

The level of RMS is slightly higher for this side of the pulley and some measurements do surpass 4,5 mm/s which is the ISO-standard reference (see Figure 38 below). This is not surprising as the back of the pulley is the side connected to the motor and is therefore affected by the motor vibrations to a greater extent. Kurtosis does seem to follow the different condition but in the opposite way of what is expected with ‘good’ measurements having high kurtosis and ‘bad’ measurements having low kurtosis.

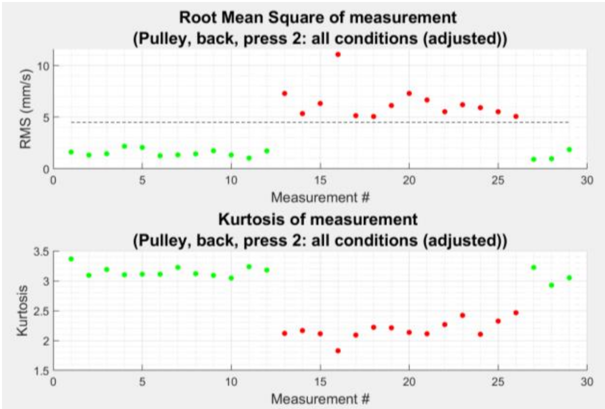

Figure 39. Statistical features with adjusted output for each measurement of the back sensor on the pulley of press 2. Upper figure: RMS of velocity. Dashed line in figure is the ISO-limit 4,5 mm/s. Lower figure: Kurtosis.

4.4.2.2 Press 4

This component has no known/no change of condition (output) and all measurements are therefore initially assumed 'decent'.

The amplitude of the FFT peaks at 25 Hz seen in Figure 41 below are quite high, higher than most 'bad' peaks at the back of the pulley on press 2. Along with a high level of RMS and PSD (Figure 40 and Figure 42 below) this implies that the condition is 'bad' for all measurements taken. Albeit again kurtosis does not provide any real information.

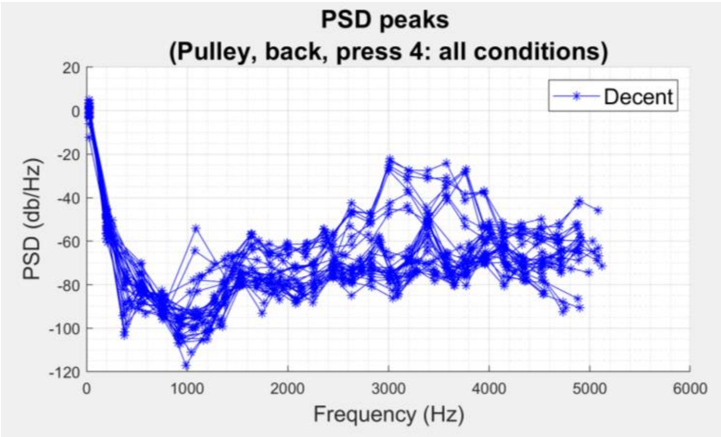

Figure 40. Distribution of PSD peak. All measurements are from the back sensor on the pulley of press 4.

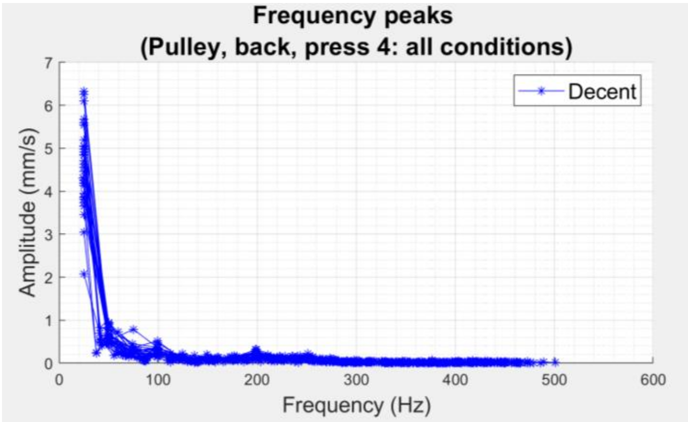

Figure 41. Distribution of FFT peaks. All measurements are from the back sensor on the pulley of press 4.

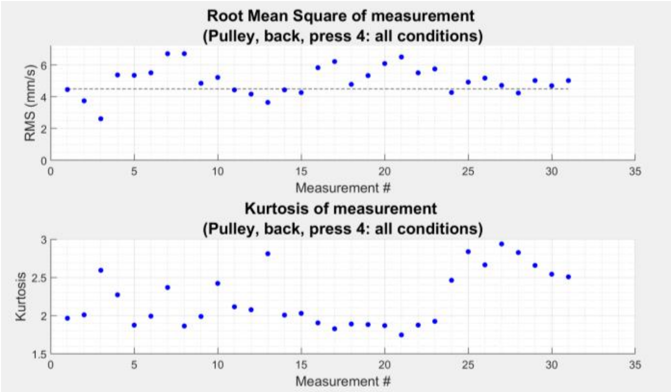

Figure 42. Statistical features for each measurement of the back sensor on the pulley of press 4. Upper figure: RMS of velocity. Dashed line in figure is the ISO-limit 4,5 mm/s. Lower figure: Kurtosis.

4.5 Gearbox

4.5.1 Front sensor

4.5.1.1 Press 2

This component has known/different conditions (outputs) and all measurements are therefore initially labelled accordingly.

The PSD in Figure 43 below shows a large gap between the level of 'good' and 'bad' measurements. The increase is rather significant, being almost 50 dB in some places. However, there are some measurements that lie in the space between the 'bad' and the lower 'good', these are adjusted to a 'decent' condition to test if this matches well with the FFT and statistical measurements (see adjusted results in Figure 44, Figure 45 and Figure 46 below).

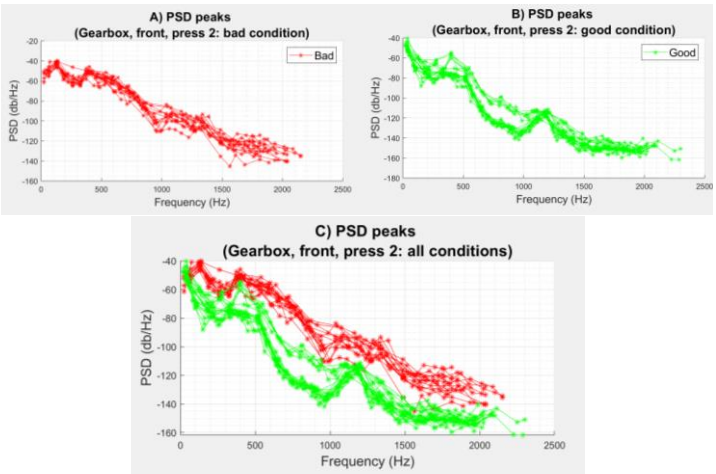

Figure 43. Distribution of PSD peaks for different conditions. All measurements are from the front sensor on the gearbox of press 2.

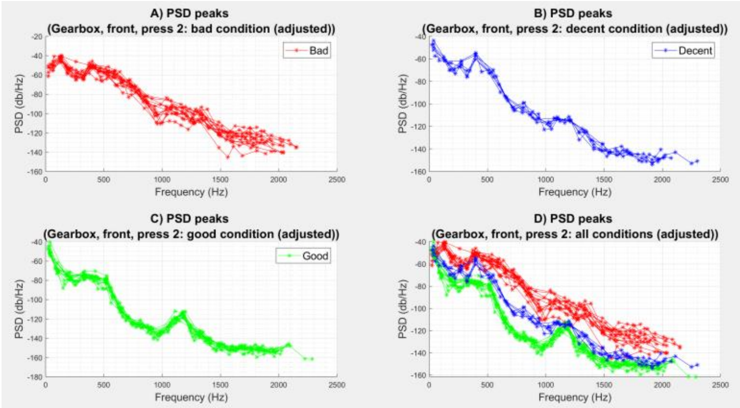

Figure 44. Distribution of PSD peaks for different conditions with adjusted output. All measurements are from the front sensor on the gearbox of press 2.

Looking at the plots in Figure 45 below it seems it was correctly assumed that the different PSD levels and assumed conditions correlates to different patterns of the FFT. These patterns and peaks may tell what the issue is with the gearbox at the time the ‘bad’ measurements were taken. For example, a peak at ~132 Hz is prevalent for a ‘bad’ condition. There are peaks around this frequency for both ‘good’ and ‘decent’ condition too, indicating that the peak has something to do with the running speed of the pinion. There are also harmonics of this frequency at ~264 Hz and ~396 Hz that are clearly visible on the graph of the ‘decent’ condition (Figure 45 B) below) and are also present for ‘bad’ condition. If the assumption that the 132 Hz peak is corresponding to the running speed, then the high amplitude at 1x might mean unbalance or an eccentric rotor. It is known that there were brass shavings from a bushing found in the crown during inspection before overhauling, there might be a connection. Large peaks might also be connected to the gear mesh frequency but (depending on the number of teeth) these tend to be at a higher frequency.

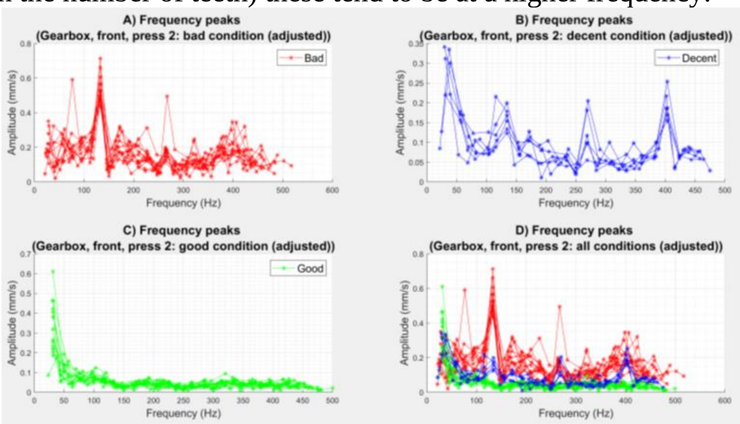

Figure 45. Distribution of FFT peaks with adjusted output for different conditions. All measurements are from the front sensor on the gearbox of press 2.

Also, the RMS shows a slight difference for the different conditions. Although the limit should be lowered to a much lower amplitude (Figure 46 below).

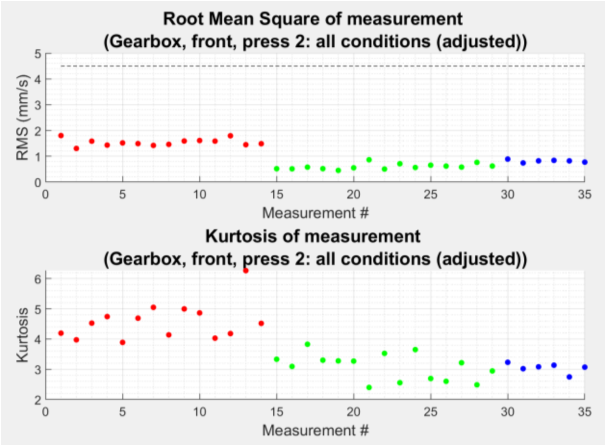

Figure 46. Statistical features with adjusted output for each measurement of the front sensor on the gearbox of press 2. Upper figure: RMS of velocity. Dashed line in figure is the ISO-limit 4,5 mm/s. Lower figure: Kurtosis.

4.5.1.2 Press 4

This component has no known/no change of condition (output) and all measurements are therefore initially assumed 'decent'.

Compared to the front of the gearbox on press 2 the PSD (compare Figure 47 above and Figure 49 below) and the FFT (compare Figure 48 above and Figure 50 below) are at low levels.

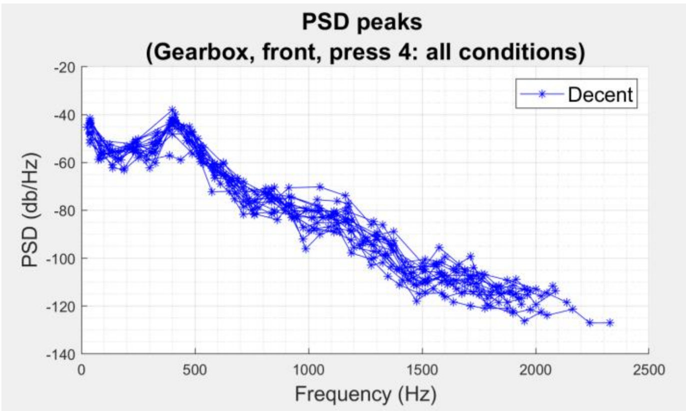

Figure 49. Distribution of PSD peaks. All measurements are from the front sensor on the gearbox of press 4.

Surprisingly there is no clear peak in the FFT at around ~135 Hz as one would expect but there are ones around 37.5 Hz. This might mean that the sensors have been mixed up in processing and this data is from the back of the gearbox, or the sensors have been reversed on press 2.

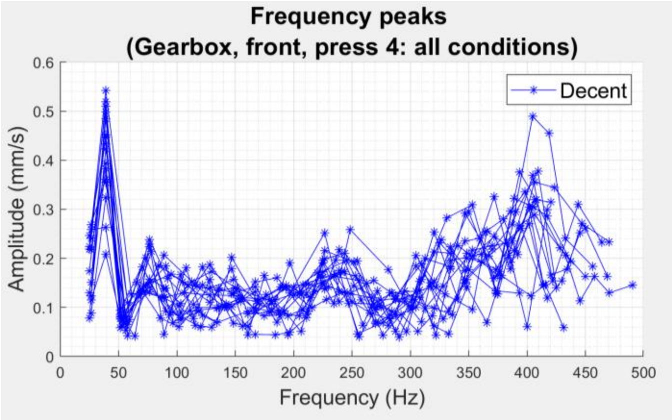

Figure 50. Distribution of FFT peaks. All measurements are from the front sensor on the gearbox of press 4.

RMS is at a low and steady level (Figure 51 below) but kurtosis is at alarming levels. This may be due to issues when measuring the vibrations, causing disturbances in the signal or issues with calculations.

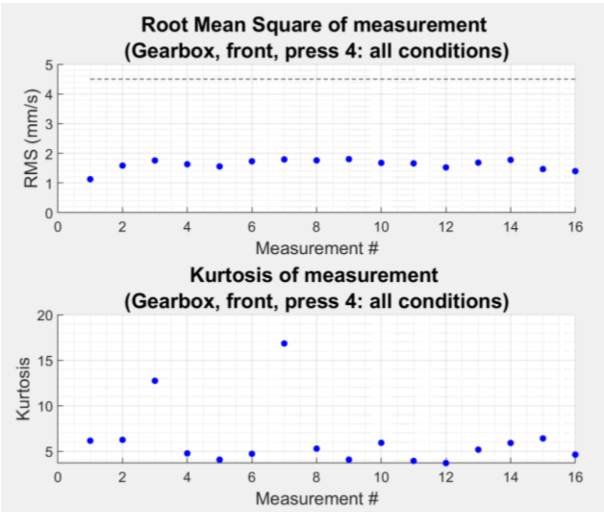

Figure 51. Statistical features for each measurement of the front sensor on the gearbox of press 4. Upper figure: RMS of velocity. Dashed line in figure is the ISO-limit 4,5 mm/s. Lower figure: Kurtosis.

4.5.2 Back sensor

4.5.2.1 Press 2

This component has known/different conditions (outputs) and all measurements are therefore initially labelled accordingly.

The measurements from the back sensor of the gearbox on press 2 are not all taken at the same time as those on the front. There are also no measurements of a 'decent' condition.

From the PSD in Figure 52 below we can gather that the general level of 'good' is lower than 'bad' between 1000-1500 Hz although the entire curve is higher in level than that on the front, which is also reflected in the RMS (Figure 55 below) where the 'bad' measurements are at the same level as the 'good' measured at the front.

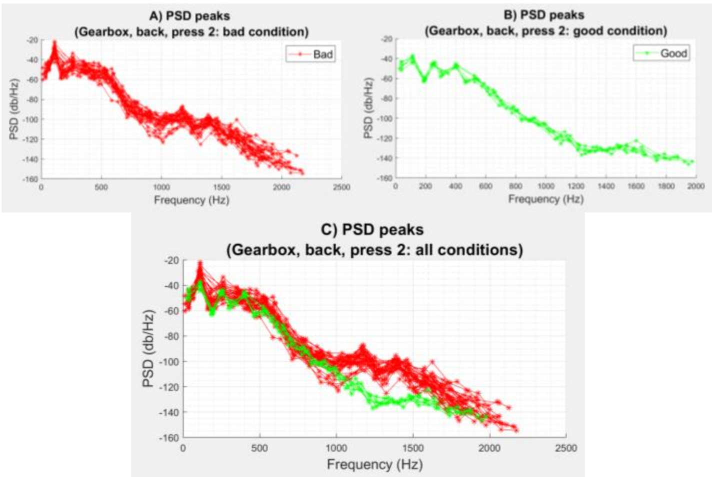

Figure 52. Distribution of PSD peaks for different conditions. All measurements are from the back sensor on the gearbox of press 2.

The ‘good’ measurements at the back also seem to be at approximately the same level as the ‘bad’ which is not surprising when looking at the FFT in Figure 53 below. The ‘good’ peaks are similar in pattern to the ‘bad’ and once again there are clear peaks at ~132 Hz and the harmonics ~154 Hz and ~402 Hz. The amplitude of these are generally higher than those at the front.

There is also reoccurring peaks at ~37.5 Hz. This might be the output (large gear) RPM.

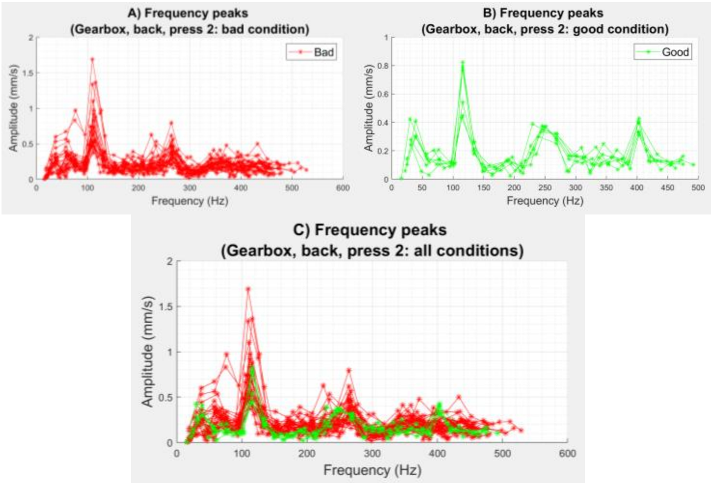

Figure 53. Distribution of FFT peaks for different conditions. All measurements are from the back sensor on the gearbox of press 2.

Kurtosis in Figure 54 below is generally somewhat lower for ‘good’ measurements but should not be solely relied upon as it is irregular.

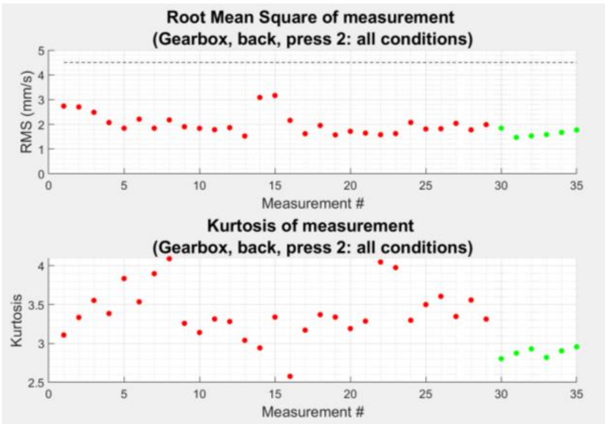

Figure 55. Statistical features for each measurement of the back sensor on the gearbox of press 2. Upper figure: RMS of velocity. Dashed line in figure is the ISO-limit 4,5 mm/s. Lower figure: Kurtosis.

4.5.2.2 Press 4

No measurements from this sensor exists at the time of the initial analysis.

4.6 Secondary axle back

4.6.1 Left side

The secondary axle is the only component that is entirely within the press crown. This component is very hard to inspect using ocular methods as the visibility is low. It is therefore of the outmost interest to see if vibration analysis is useful for condition monitoring of the secondary axle.

4.6.1.1 Press 2

This component has known/different conditions (outputs) and all measurements are therefore initially labelled accordingly.

The pattern of the PSD on the left secondary axle of press 2 is very similar to the pattern of the PSD for the front sensor on the gearbox of press 2 (compare Figure 42 above and Figure 56 below). Although the PSD of the axle seen below shows higher levels. Once again there is also some measurements that lie inbetween the 'bad' and the lower pattern of 'good'.

The condition of these is adjusted to 'decent' (see adjusted PSD in Figure 57).

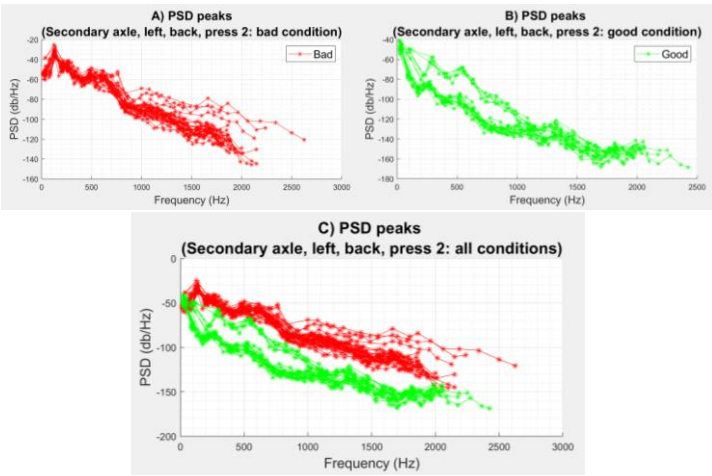

Figure 56. Distribution of PSD peaks for different conditions. All measurements are from the back sensor on the left secondary axle of press 2.

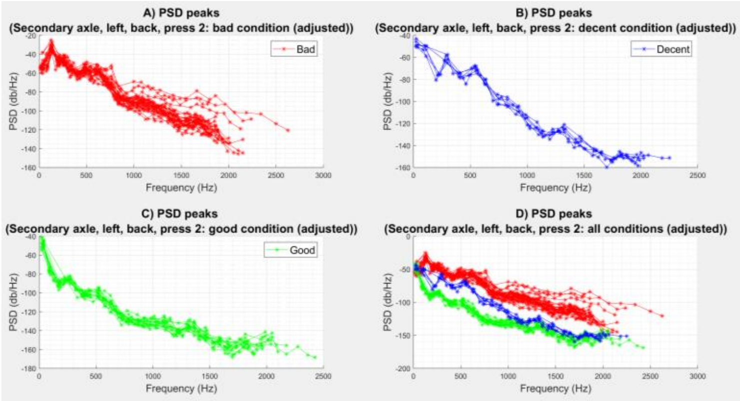

Figure 57. Distribution of PSD peaks for different conditions with adjusted output. All measurements are from the back sensor on the left secondary axle of press 2.

Now looking at the adjusted FFT and RMS/Kurtosis (Figure 58 and Figure 59 below) the adjusted output seems to make sense as the adjusted measurements have a different pattern of peaks in FFT and the RMS is slightly higher than the 'good'. The level of kurtosis does follow the different conditions quite well but should not be solely relied upon as it is irregular. Although, the average level of kurtosis for the different conditions do seem to create different levels, meaning that kurtosis should, if used, be used as the average of several measurements.

The FFT is very similar to the front gearbox FFT and so is the RMS. This might mean that these two sensors are picking up the same things.

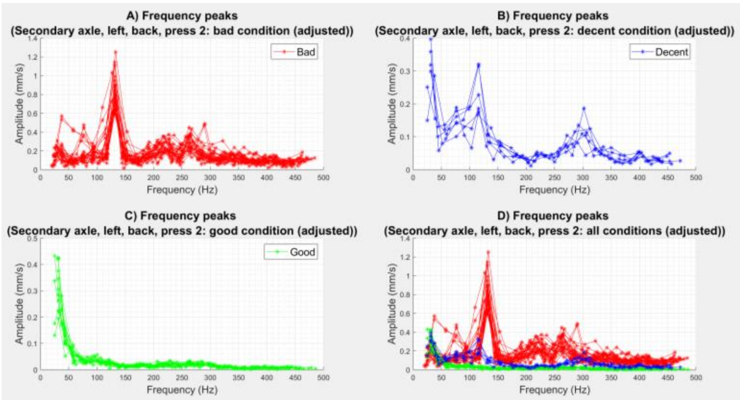

Figure 58. Distribution of FFT peaks with adjusted output for different conditions. All measurements are from the back sensor on the left secondary axle of press 2.

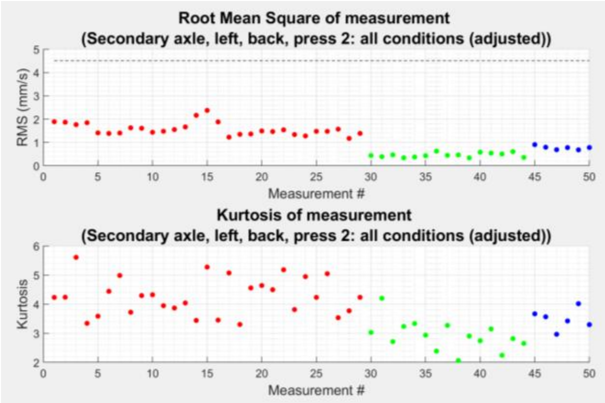

Figure 59. Statistical features with adjusted output for each measurement of the back sensor on the left secondary axle of press 2. Upper figure: RMS of velocity. Dashed line in figure is the ISO-limit 4,5 mm/s. Lower figure: Kurtosis.

4.6.1.2 Press 4

This component has no known/no change of condition (output) and all measurements are therefore initially assumed 'decent'.

The PSD on the left secondary axle on press 4 (Figure 60 below) is very similar to the 'decent' measurements on the same position in press 2 (Figure 57 above).

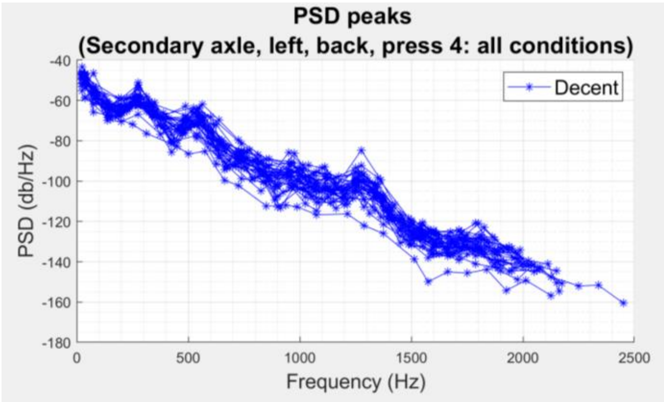

Figure 60. Distribution of PSD peaks. All measurements are from the back sensor on the left secondary axle of press 4.

However, the FFT is slightly different (compare Figure 58 above and Figure 61 below). The amplitude seen in Figure 61 is generally not higher than for press 2 but there are harmonic peaks of that are not present on press 2.

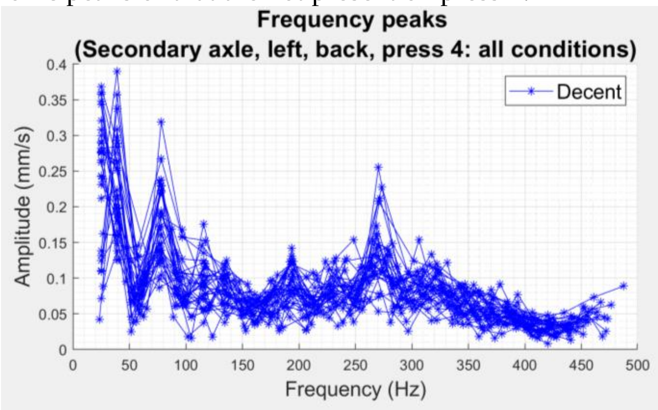

Figure 61. Distribution of FFT peaks. conditions. All measurements are from the back sensor on the left secondary axle of press 4.

The RMS is again low and even, but kurtosis is rather high and irregular with some rouge measurements (see Figure 62). In combination with the harmonics present in the FFT, high levels of kurtosis might mean that there are shocks present in the signal caused by localized faults on a gear, bearing or axle. These faults may be present and causing shocks without really starting to affect the overall vibration level (RMS).

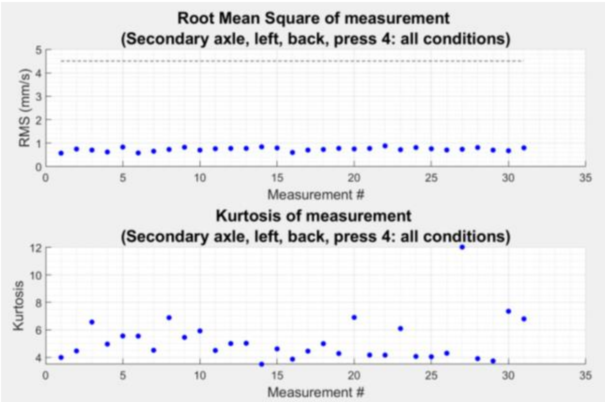

Figure 62. Statistical features for each measurement of the back sensor on the left secondary axle of press 4. Upper figure: RMS of velocity. Dashed line in figure is the ISO-limit 4,5 mm/s. Lower figure: Kurtosis.

4.6.2 Right side

4.6.2.1 Press 2

This component has known/different conditions (outputs) and all measurements are therefore initially labelled accordingly.

On the right side secondary axle the same thing is happening as on the right. Some 'good' measurements have a higher level PSD at around 500-1000 Hz (Figure 63 below). These are adjusted to 'decent' (see Figure 64).

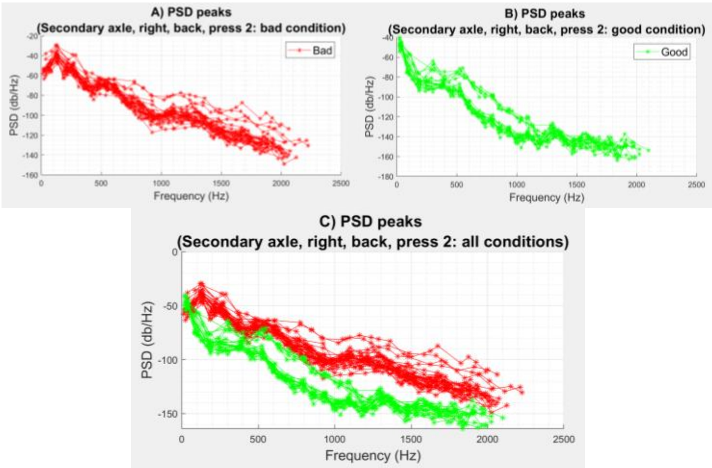

Figure 63. Distribution of PSD peaks for different conditions. All measurements are from the back sensor on the right secondary axle of press 2.

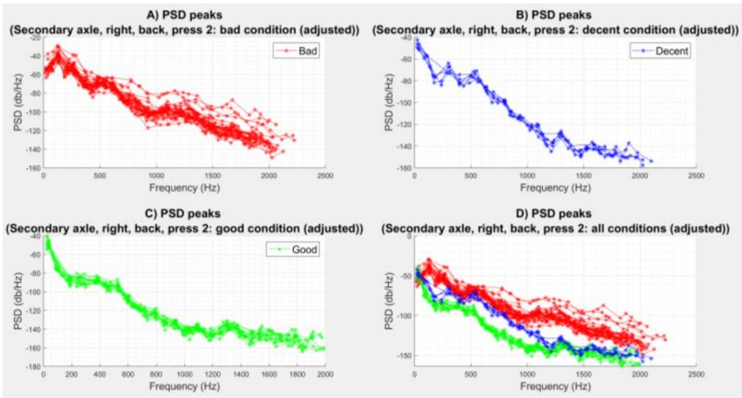

Figure 64. Distribution of PSD peaks with adjusted output for different conditions. All measurements are from the back sensor on the right secondary axle of press 2.

The results of the FFT and RMS in Figure 65 and Figure 66 below almost look copied from the back of the left secondary axle seen in Figure 57 and Figure 58. Once again raising suspicion that the sensors on the back of the secondary axle may be picking up on the same thing as the sensor on the front of the gearbox.

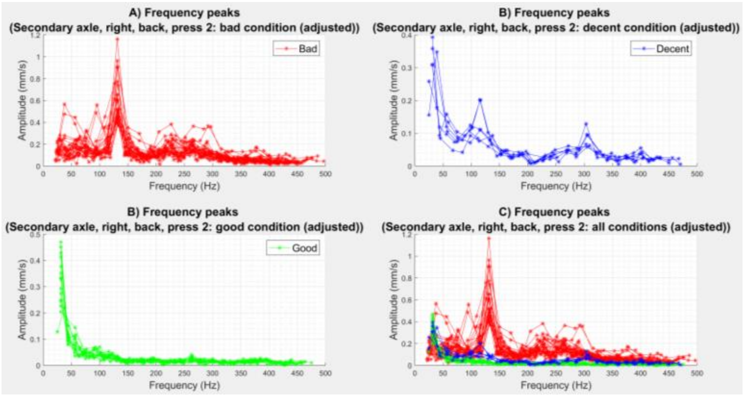

Figure 65. Distribution of FFT peaks with adjusted output for different conditions. All measurements are from the back sensor on the right secondary axle of press 2.

Once again some 'bad' measurements have a kurtosis level above the recommended limit of 4 but the measures are not consistent enough to make any conclusions.

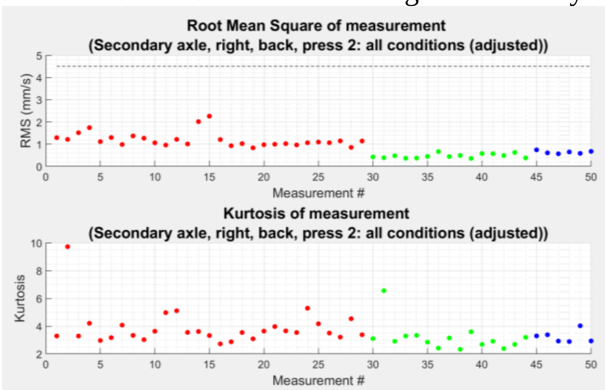

Figure 66. Statistical features with adjusted output for each measurement of the back sensor on the right secondary axle of press 2. Upper figure: RMS of velocity. Dashed line in figure is the ISO-limit 4,5 mm/s. Lower figure: Kurtosis.

4.6.2.2 Press 4

This component has no known/no change of condition (output) and all measurements are therefore initially assumed 'decent'.

The same conclusions can be made for the measurements from this sensor as the ones in 4.6.1.2 regarding PSD and RMS/kurtosis seen in Figure 67 and Figure 69 below.

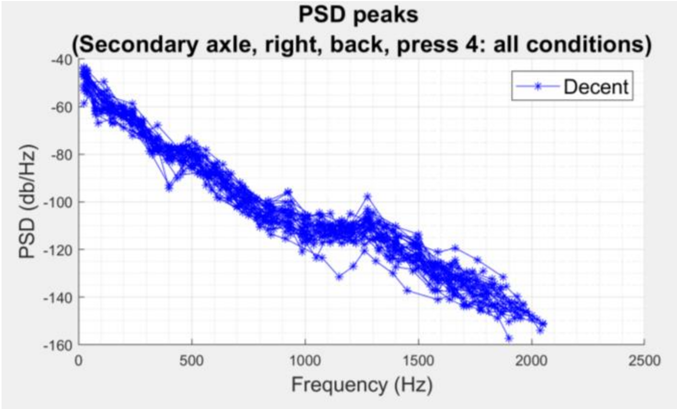

Figure 67. Distribution of PSD peaks for different conditions. All measurements are from the back sensor on the right secondary axle of press 4.

FFT shows some interesting peaks that are probably harmonics of some sort at ~39, 78, 117, 156, 195, 234, 273 and 312 Hz (see Figure 68). Harmonics in this number may mean that something is wrong. In this case it might be angular misalignment (see Appendix A).

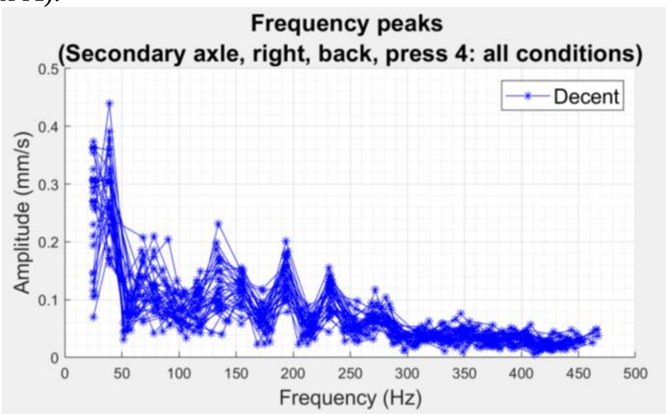

Figure 68. Distribution of FFT peaks with different output for different conditions. All measurements are from the back sensor on the right secondary axle of press 4.

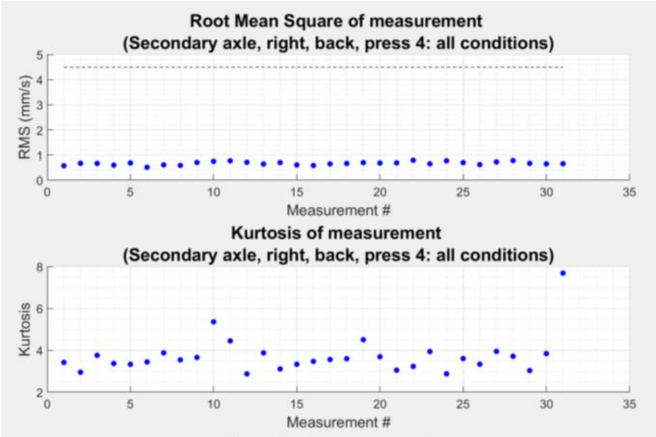

Figure 69. Statistical features for each measurement of the back sensor on the right secondary axle of press 4. Upper figure: RMS of velocity. Dashed line in figure is the ISO-limit 4,5 mm/s. Lower figure: Kurtosis.

4.7 Secondary axle front

This sensor is placed on the front end of the secondary axle near the eccentric wheel. The sensor does not necessarily pick up vibrations from the eccentric wheel, but it might be a possibility.

4.7.1 Left side

4.7.1.1 Press 2

This component has known/different conditions (outputs) and all measurements are therefore initially labelled accordingly.

The amplitude of the PSD is rather high, especially around 100-200 Hz (see Figure 70 below). This is accompanied by a high peak in the FFT at ~132 Hz (Figure 71 below). This peak also had a clear presence by the gearbox of press 2 (see Figure 45 and Figure 53 above).

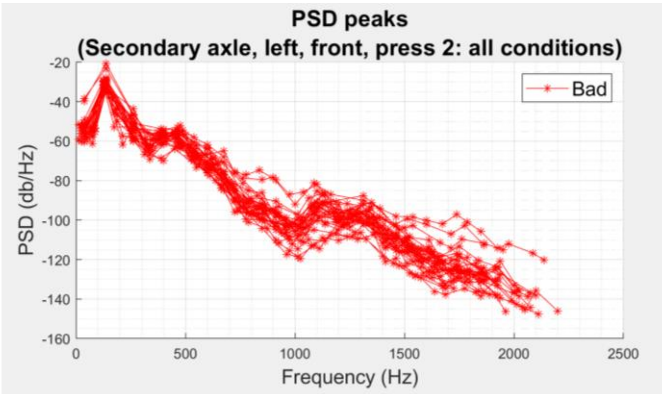

Figure 70. Distribution of PSD peaks. All measurements are from the front sensor on the left secondary axle of press 2.

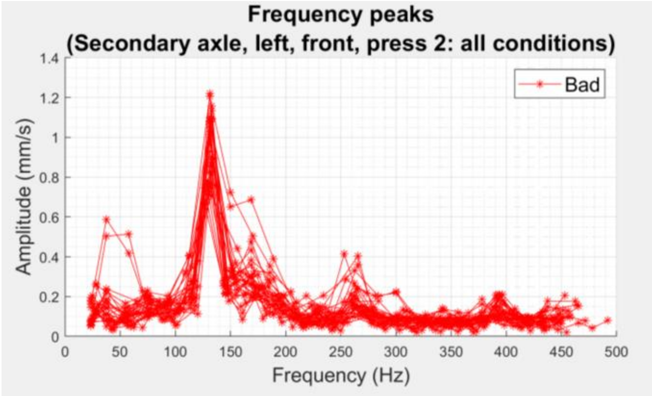

Figure 71. Distribution of FFT peaks. All measurements are from the front sensor on the left secondary axle of press 2.

RMS is higher than 1 (see Figure 72 below) which it has not been for any previously observed 'good' or 'decent' measurements of the secondary axle. Kurtosis is lower than 4 for almost all measurements which might mean that the fault has become distributed and judging by the FFT the fault might be caused the high amplitude peak at ~132 Hz.

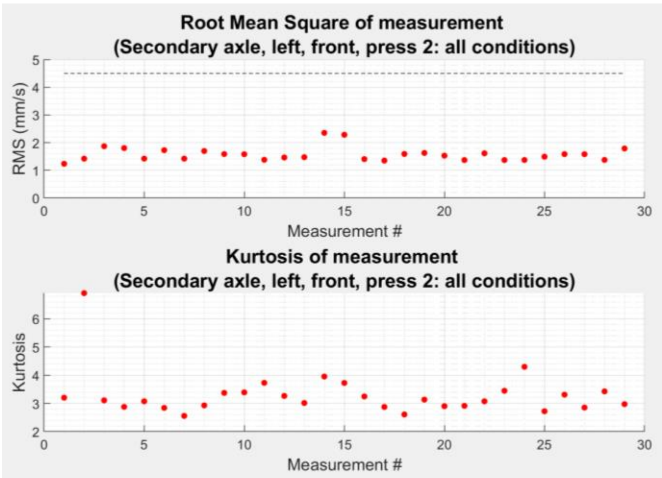

Figure 72. Statistical features for each measurement of the front sensor on the left secondary axle of press 2. Upper figure: RMS of velocity. Dashed line in figure is the ISO-limit 4,5 mm/s. Lower figure: Kurtosis.

4.7.1.2 Press 4

This component has no known/no change of condition (output) and all measurements are therefore initially assumed 'decent'.

All measures in Figure 73, Figure 74 and Figure 75 seemseem to be quite low compared to press 2 and are similar to the equivalent back sensors on the secondary axle.

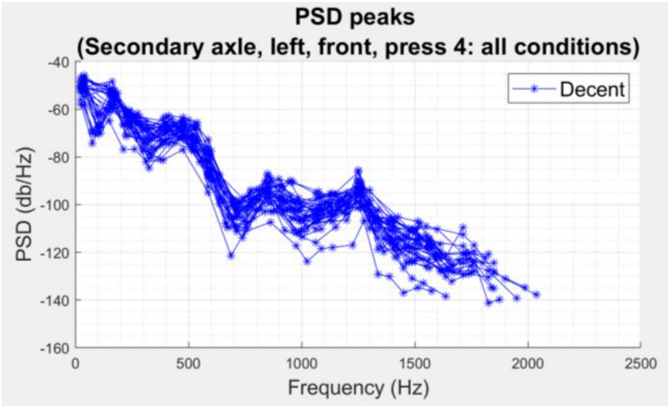

Figure 73. Distribution of PSD peaks. All measurements are from the front sensor on the left secondary axle of press 4.

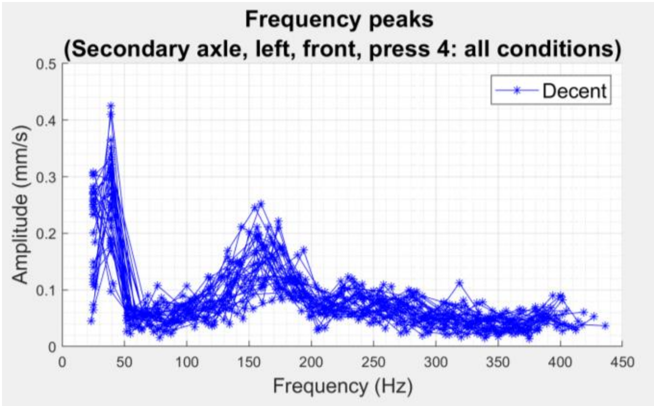

Figure 74. Distribution of FFT peaks. All measurements are from the front sensor on the left secondary axle of press 4.

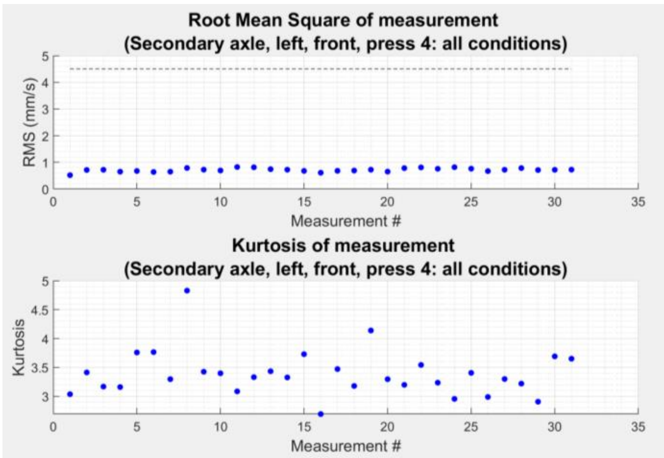

Figure 75. Statistical features for each measurement of the front sensor on the left secondary axle of press 4. Upper figure: RMS of velocity. Dashed line in figure is the ISO-limit 4,5 mm/s. Lower figure: Kurtosis.

4.7.2 Right side

4.7.2.1 Press 2

This component has known/different conditions (outputs) and all measurements are therefore initially labelled accordingly.

The output conditions are adjusted to match the conditions of the front sensor on the secondary axle as the measurements of this sensor are of the same component and taken at the same time.

The measurements are again similar to the secondary axle but the PSD level is higher around 100-200 Hz (see Figure 76).

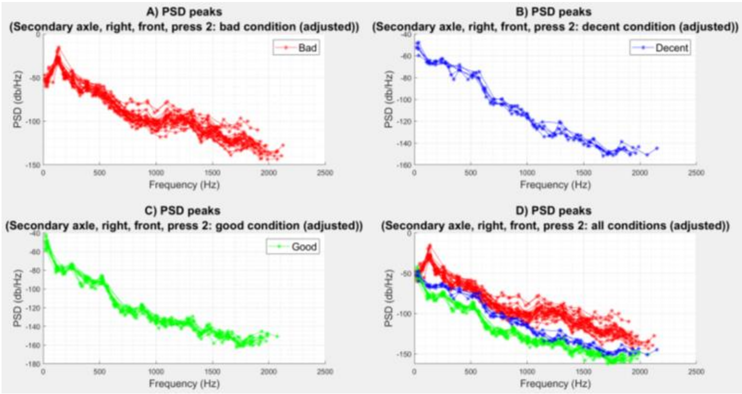

Figure 76. Distribution of PSD peaks with adjusted output for different conditions. All measurements are from the front sensor on the right secondary axle of press 2.

The peak in FFT at ~132 Hz is also present confirming that the fault is not localized to the back of the secondary axle but affects also the front sensor by the eccentric wheel (compare Figure 64 above Figure 77 below). However, the amplitude of the peak is higher by the eccentric wheel, maybe due to outside the fault being nearer this end of the axle, also making the RMS higher (see Figure 78 below).

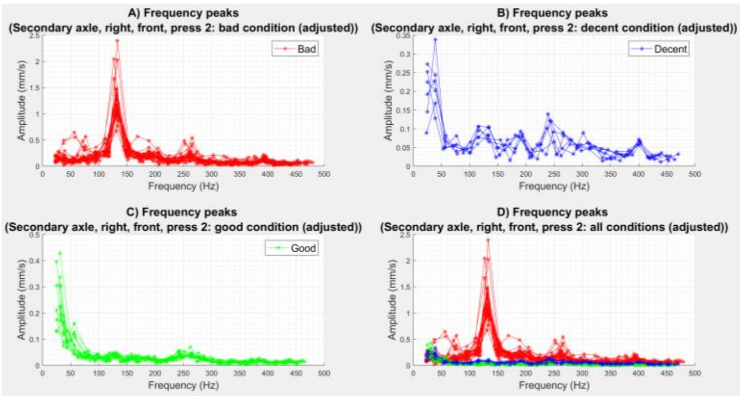

Figure 77. Distribution of FFT peaks with adjusted output for different conditions. All measurements are from the front sensor on the right secondary axle of press 2.

Kurtosis does not provide any direct information about the condition. Just as on the left side the low level of kurtosis for ‘bad’ measurements may be due to localized fault becoming distributed. This also means that the level of kurtosis might have been higher levels in earlier measurements before dropping to the level seen in Figure 78 below.

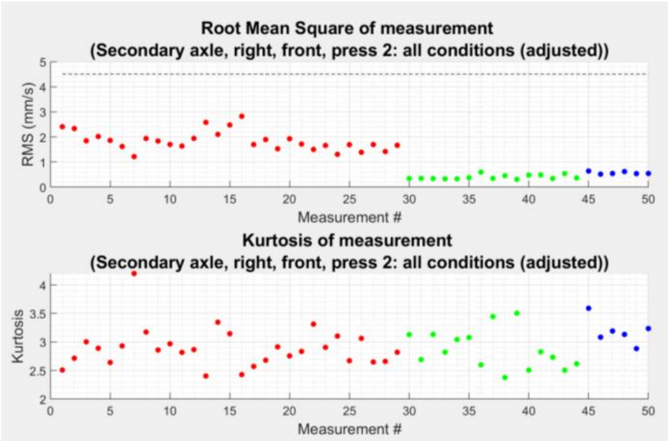

Figure 78. Statistical features for each measurement of the front sensor on the right secondary axle of press 2. Upper figure: RMS of velocity. Dashed line in figure is the ISO-limit 4,5 mm/s. Lower figure: Kurtosis.

4.7.2.2 Press 4

This component has no known/no change of condition (output) and all measurements are therefore initially assumed ‘decent’.

All measures in Figure 79, Figure 80 and Figure 81 seem to be quite low compared to the corresponding measurements on press 2 and are similar to the equivalent back sensors on the secondary axle found in 4.7.2.2.

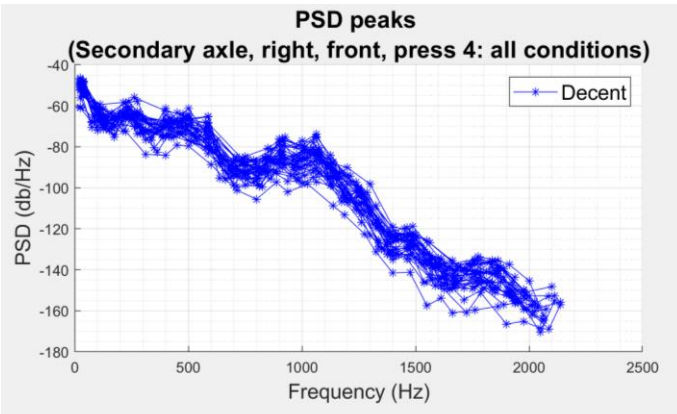

Figure 79. Distribution of PSD peaks. All measurements are from the front sensor on the right secondary axle of press 4.

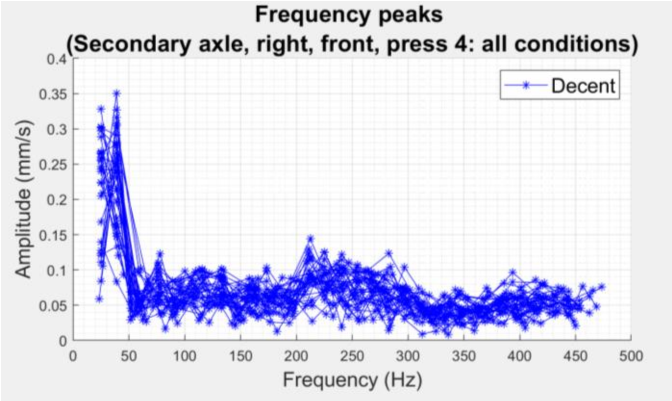

Figure 80. Distribution of FFT peaks. All measurements are from the front sensor on the right secondary axle of press 4.

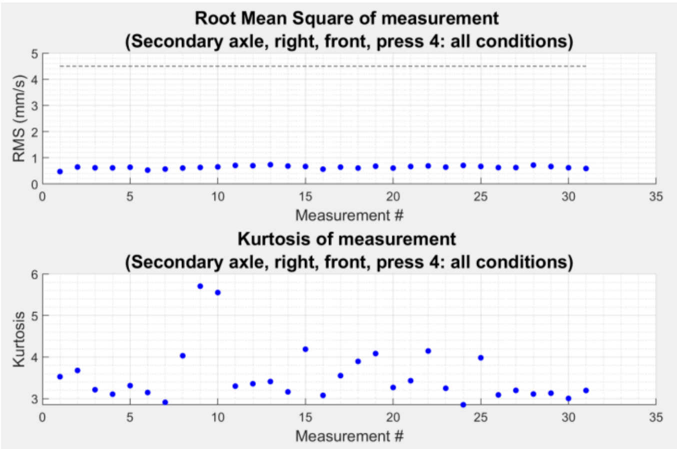

Figure 81. Statistical features for each measurement of the front sensor on the right secondary axle of press 4. Upper figure: RMS of velocity. Dashed line in figure is the ISO-limit 4,5 mm/s. Lower figure: Kurtosis.

4.8 Comparison with new measurements

Some new measurements from March/April 2019 are compared to the initial measurements from earlier in this chapter. This comparison will act as an initial verification of some prior assumptions with regards to the usefulness of vibration analysis in these applications. Not all components will be compared this way, instead only some of the components that provided much information during initial analysis and its counterpart on the other press, will be compared.

4.8.1 Motor front/back

Does not contain useful information, excluded from report.

4.8.2 Pulley front

4.8.2.1 Press 2

As this sensor has previously recorded many different conditions, it is interesting to see if any new measurments follow the same pattern. Judging from Figure 82, Figure 83 and Figure 84 below the new measurments do correspond well to the pattern of a ‘good’ condition. Unfortunately this does not answer the question of different faults show different spectral signatures in the PSD or FFT.

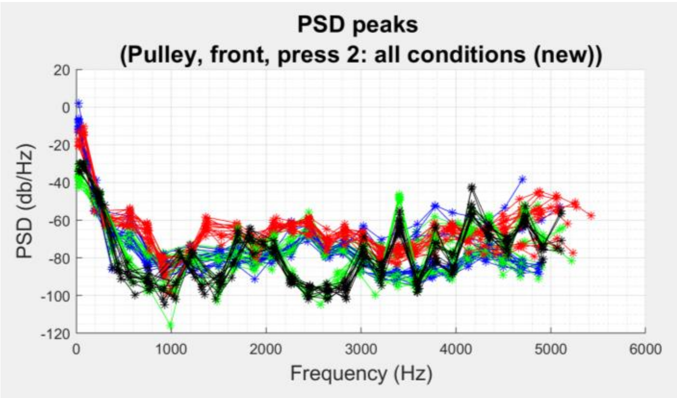

Figure 82. Comparison of the distribution of PSD peaks for different conditions. All measurements are from the front sensor on the pulley of press 2. New measurements in black.

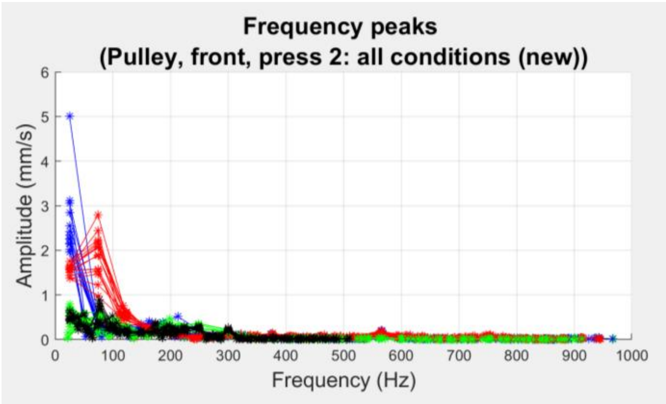

Figure 83. Comparison of the distribution of FFT peaks for different conditions. All measurements are from the front sensor on the pulley of press 2. New measurements in black.

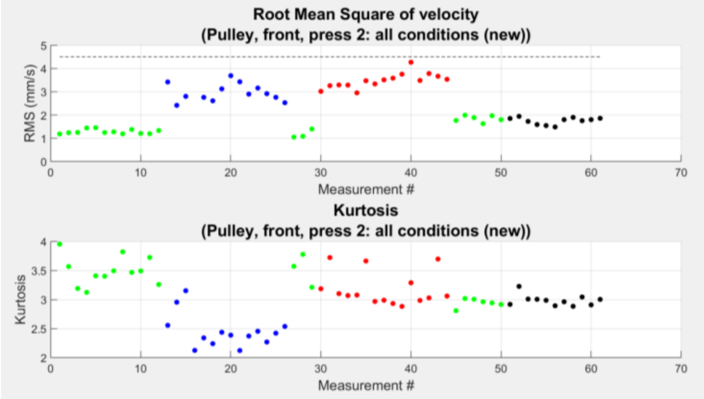

Figure 84. Comparison of the distribution of statistical measures RMS (upper figure) and kurtosis (lower figure) for different conditions. All measurements are from the front sensor on the pulley of press 2. New measurements in black.

4.8.2.2 Press 4

Does not contain useful information, excluded main report.

4.8.3 Pulley back

4.8.3.1 Press 2

There are currently no new measurements.

4.8.3.2 Press 4

Does not contain useful information, excluded from report.

4.8.4 Gearbox Front

4.8.4.1 Press 2

Does not contain useful information, excluded from report.

4.8.4.2 Press 4

Judging from the results in Figure 85, Figure 86 and Figure 87 below the condition at the front of the gearbox on press 4 is worse than it was when the first measurements were taken. The overall level of PSD and RMS has significantly increased and the FFT shows very irregular peaks which might be indicating internal looseness or be due to gearing issues.

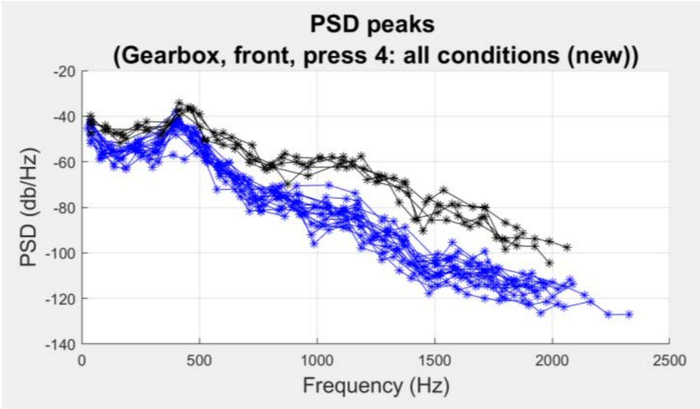

Figure 85. Comparison of the distribution of PSD peaks. All measurements are from the front sensor on the gearbox of press 4. New measurements in black.

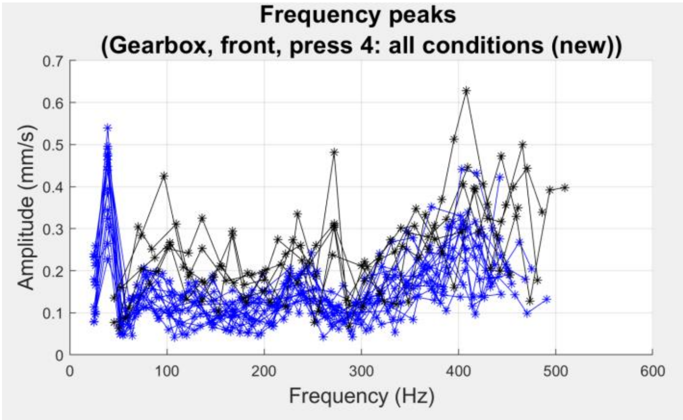

Figure 86. Comparison of the distribution of FFT peaks. All measurements are from the front sensor on the gearbox of press 4. New measurements in black.

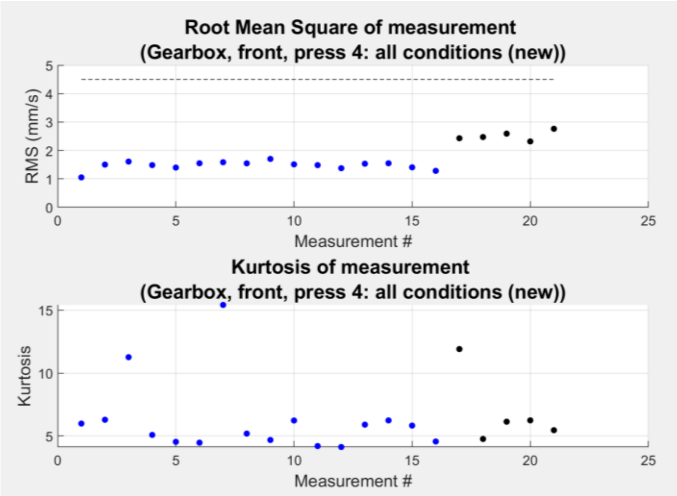

Figure 87. Comparison of the distribution of statistical measures RMS (upper figure) and kurtosis (lower figure). All measurements are from the front sensor on the gearbox of press 4. New measurements in black.

4.8.5 Gearbox back

4.8.5.1 Press 2

Does not contain useful information, excluded from report.

4.8.5.2 Press 4

There are no previous measurments from the back of the gearbox on press 4 but levels in Figure 88, Figure 89 and Figure 90 below are generally high. Judging from prior results from the gearbox on press 2, the vibrations at the front and back of a gearbox seem to follow eachother quite well and it is theefore not surprising that the new measurements at the front and back seem to indicate that something is wrong even though the fault might be localized.

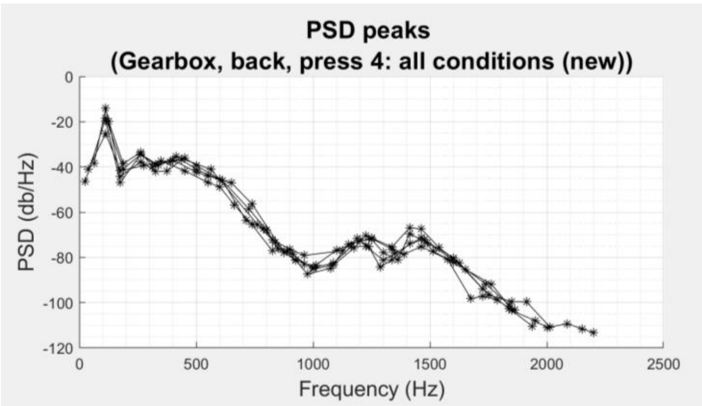

Figure 88. Comparison of the distribution of PSD peaks. All measurements are from the back sensor on the gearbox of press 2. All new measurements.

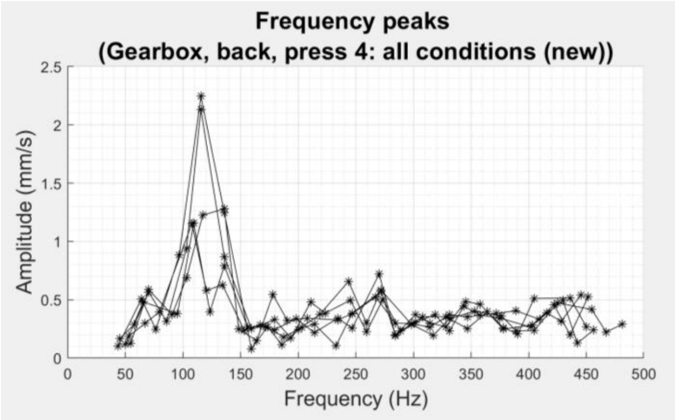

Figure 89. Comparison of the distribution of FFT peaks. All measurements are from the back sensor on the gearbox of press 4. All new measurements.

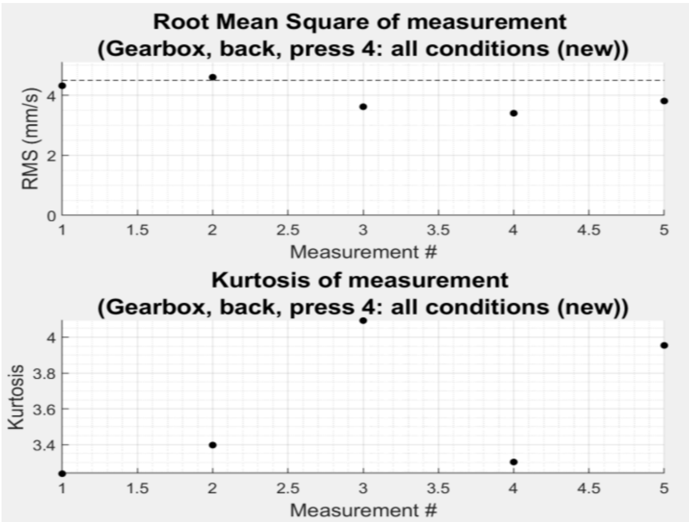

Figure 90. Comparison of the distribution of statistical measures RMS (upper figure) and kurtosis (lower figure). All measurements are from the back sensor on the gearbox of press 4. All new measurements.

4.8.6 Left Secondary axle front

4.8.6.1 Press 2

There are currently no new measurements.

4.8.6.2 Press 4

As with the new measurements of the gearbox on press 4 the general level in Figure 91, Figure 92 and Figure 93 below is higher than before. The level of RMS has not increased as much but as the RMS alarm-level for this components has yet to be established (the dotted line at 4,5 mm/s is just a point of reference and there are no specific ISO-guidelines for this component at this time), the slight increase might be enough to raise alarm. The increase might also imply that the general level of noise in the crown of press 4 has increased.

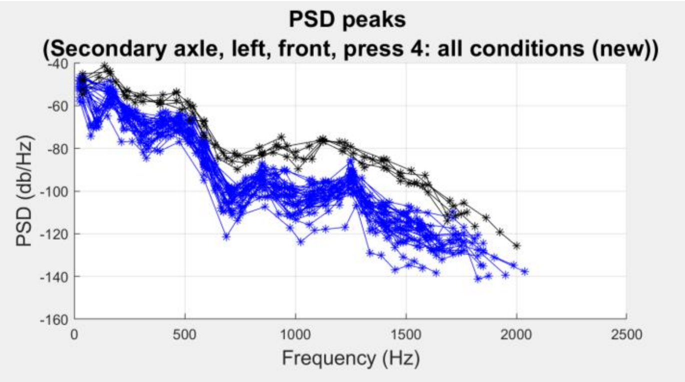

Figure 91. Comparison of the distribution of PSD peaks. All measurements are from the front sensor on the left secondary axle of press 4. New measurements in black.

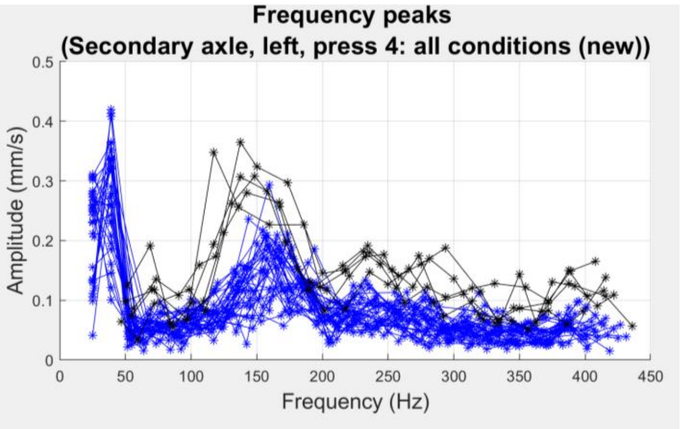

Figure 92. Comparison of the distribution of FFT peaks. All measurements are from the front sensor on the left secondary axle of press 4. New measurements in black.

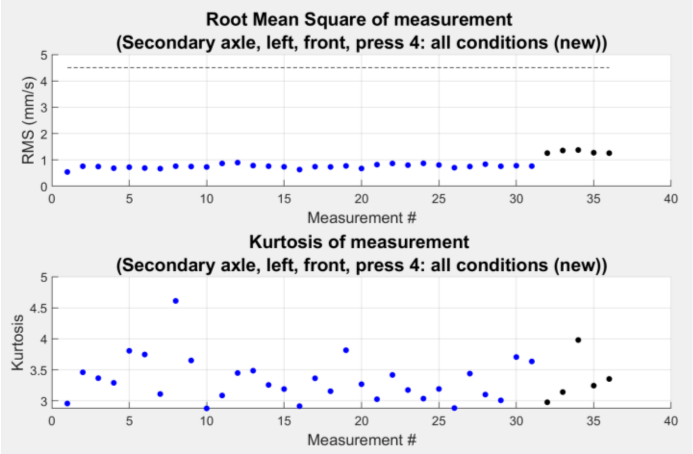

Figure 93. Comparison of the distribution of statistical measures RMS (upper figure) and kurtosis (lower figure). All measurements are from the front sensor on the left secondary axle of press 4. New measurements in black.

4.8.7 Left secondary axle back

4.8.7.1 Press 2

Does not contain useful information, excluded from report.

4.8.7.2 Press 4

Does not contain useful information, excluded from report.

Same conclusion as the front sensor on the same component found in 4.8.6.2.

4.8.8 Right secondary axle front

4.8.8.1 Press 2

Does not contain useful information, excluded from report.

4.8.8.2 Press 4

Does not contain useful information, excluded from report.

Same conclusion as the corresponding sensor on the left secondary axle found in 4.8.6.2.

4.8.9 Right secondary axle back

4.8.9.1 Press 2

Does not contain useful information, excluded from report.

4.8.9.2 Press 4

Does not contain useful information, excluded from report.

Same conclusion as the corresponding sensor on the left secondary axle found in 4.8.6.2.

4.9 Machine learning trial

Using measurements from the front sensor of the pulley of press 2 where there are many different outputs, it is possible to use supervised learning and classification to test if machine learning is suitable for implementation.

It is possible to choose which features that should be included when training the model. If the amplitude of the first two peaks of the FFT and the RMS is used for training, the model accuracy may reach 100%. Using this model when classifying the new data from 4.8.2.1 it will classify all new measurements as ‘good’ which does seem accurate based on the result in Figure 82-83. When running measurements from the front sensor of the pulley on press 4 the predicted output does not correspond as well with previous assumptions.

Using only the two first FFT peak amplitudes as predictive features also generates a 100% prediction accuracy and ‘good’ predictions of the new measurements. Meaning the model might be over defined when also using RMS as a predictive feature. Only using the RMS however does only reach 90% model accuracy meaning the model is underdefined.

Training a model using the amplitude of the first peak collected from the PSD and the RMS generates 98% prediction accuracy, with one ‘decent’ measurement being classified as ‘bad’. But all new measurements are classified as ‘good’ as with using FFT-predictors. It is difficult using any other PSD-peaks than the first one at this stage as the peaks have not been sorted so all the peak values in the same feature correspond to the same frequency. If the peaks are extracted in a different way, for example peaks are extracted for certain frequencies or sorted based on the frequencies, then it might be better using PSD- than FFT-peaks as predictive features. As it is now, the FFT is better to use as it seems to generate peaks at recurring frequencies.

Repeating the same procedure using the measurements from the front sensor on the right secondary axle of press 2, it is possible to get 100% accuracy using the second and fourth peak level of the PSD. Using this model, the new measurements are classified as ‘good’ or ‘decent’ and the measurements from the corresponding sensor on press 4 are classified similarly to what was previously assumed. The new measurements on press 4 are classified mostly as ‘bad’ which also resonates with assumptions.

Using the amplitude of the fifth and seventh FFT-peaks as predictive features it is also possible to get 100% accuracy and the classification of the new measurements and measurements from press 4 is like the earlier results when using PSD-features to train the model.

5 Discussion

- *Can vibration analysis be used for predictive maintenance of a mechanical press in the sense of fault detection and fault analysis?*

Judging from the extensive analysis performed in the previous chapter, vibrations can be used for fault detection by monitoring the overall vibration level through RMS or using frequency domain measures like PSD to monitor the increase of vibrations in certain frequency intervals. Yet both these methods will require a baseline value be set to which all new measurements can be referred.

Regarding fault diagnosis; the assumptions regarding diagnosis made in the previous chapter will have to be confirmed to say whether diagnosis using FFT is possible in this case. Establishing the actual diagnosis may also provide information about which peaks in the FFT are caused or heightened by that particular fault, which may enable FFT to be used for more precise condition monitoring and diagnostics on that component in the future.

Assumptions regarding past conditions might be difficult to confirm but the present condition of for example the gearbox or the left secondary axle of press 4 have new measurements with high level vibrations and the present condition can be checked to see if it correlates to the analysis.

Also, based on similar applications found during theoretical research, the application of vibration analysis on complex machinery has been proved possible for example on cold roll presses for aluminium and in the paper industry.

- *Which means of analysis provides necessary information about the condition of different components?*

RMS seem to provide some information about the condition and could possibly be used for fault detection. In this thesis the RMS value is calculated from the interval 20-2000 Hz of the FFT, a larger interval might provide even more information about faults that show up as high frequency peaks like issues with gears or bearings. Also, most of the ‘bad’ measurements that have been recorded have been caused by relatively severe faults and components that are very near failure. At this stage it is expected that the overall vibration level (measured by RMS) is high but for predictive maintenance to work the fault need to be caught before the condition is critical. Due to not having enough data from a condition that is known to be bad but not critical it is hard to say if RMS will give proper warning at that stage.

Kurtosis generally shows no real reliability in fault detection purposes. The measure was calculated from the filtered velocity signal which might contain amplified noise, causing irregularities. It should be noted however, that kurtosis does provide some useful information in the monitoring of the gearbox, where kurtosis-measures of different conditions seem to gather around different levels. This would mean that to monitor kurtosis the mean value of several measurements would have to be trended and monitored.

Using PSD for condition monitoring does require knowledge about the baseline PSD at a well-established normal/good condition OR thorough knowledge about the current state of the component. Not to cause data overload by monitoring the entire spectra, some specific lines to monitor must be chosen. To decide which spectral lines or intervals that need to be monitored, further testing should be done to establish if different faults will cause heightened levels in the same interval of frequencies. Judging from the comparison made with new measurements, new measurements have similar PSD patterns. Another possible action is lowering the resolution of the PSD to gather information about a wider bandwidth of frequencies at each spectral line.

- *How to interpret collected vibration data in an analysis.*

How to interpret the vibrations data has been discussed throughout the analysis. Assumptions about what the varying levels and peaks in the PSD/FFT might imply has also been discussed but must be confirmed. How to interpret peaks in the FFT can be found in Appendix A.

- *How much information will vibration analysis provide about the condition?*

It seems vibration analysis could be used to at least tell if the condition is 'good', 'decent' or 'bad'. If a diagnosis can be made when only provided with vibration data is still unknown at this time. For the time being, vibration analysis should only act as an extra input to go along with maintenance being performed as it is now. This will also mean that the use of vibration analysis will be put through trial-and-error and any results of analysis validated.

- *Is vibrational information exchangeable between corresponding components on different equipment?*

It is hard to draw conclusions around whether similar component on different presses have similar vibration signatures. Looking at the PSD and FFT of the sensors on the secondary axle of press 2 and press 4 these are quite like each other. But although patterns and levels may be similar between some corresponding components, all should be treated individually to establish that particular component's baseline. Same goes for when a component has been exchanged or thoroughly refurbished. As previously mentioned, a mechanical press is a complex machinery and there are many things that will affect the emitted vibrations.

- *Also, would it be possible to use machine learning for conditions monitoring in this application?*

Initial trials show that using carefully selected predictive features may generate models that achieve 100% accuracy in training. These models also seem to make realistic predictions of new data. Which features are best used as predictors depends on the component in question, but PSD, FFT and RMS all seem useful.

It might be necessary to look at new ways of generating features to get the best result, extracting the PSD-level at certain frequencies or sorting the FFT-amplitudes based on frequency might prove crucial in making good machine-learning models.

- *Discussion of further questions:*

Measuring vibrations only when running the same job is probably a good choice. When doing so, the average level of the measurements will change more between each set of measurements (between each time that job is run) and make it easier to distinguish changes. Like the way measurements were analysed in this thesis.

Another benefit of this approach is that data acquisition and calculations do not have to be run simultaneously and continuously. Although a cloud solution might be a viable option for data storage and handling in the future it will probably not be necessary during trial-and-error.

Also, performing measurements only during the same job will eliminate one variable that might affect the result, reducing the complexity of the problem.

It was previously mentioned that a small segment at the start of the raw signal had to be cut out when integrating to velocity. When integrating, some irregularities may become amplified causing great shocks and high amplitude peaks in the integrated signal. When analysing rotating components, the signal behaviour should be periodic, and any shocks due to damage on the rotating component should be present in each revolution. In this case there were large aperiodic shocks at the beginning of the integrated signal and it therefore had to be cropped out. This behaviour might be due to the component not having time to stabilize. For example, the motor is analysed during "idle" operation i.e. when the clutch is not engaged but this segment of time follows directly after a press stroke when the clutch and brake will affect the motor vibrations, causing variations and increases. By cropping out this part of the signal the result will be much more reliable as to monitoring the condition of the motor.

6 Conclusion

In this thesis the prospect of using vibrations to analyse the condition and possible diagnose mechanical presses was researched. Analysis was done by comparing some randomly chosen measurements from different dates and assigning them with one of three outputs ‘good’, ‘decent’ or ‘bad’.

The goal was to establish if the spectral methods PSD and FFT, RMS or statistical measure kurtosis would provide information that made each condition distinguishable.

The following conclusions were made:

- Vibration analysis can be used in predictive monitoring of mechanical presses.
- RMS does seem to work for fault detection but should be complemented with some form of spectral analysis.
    - Furthermore, RMS should be calculated from the FFT of a carefully chosen interval of frequencies and not from the overall time domain signal.
- The usefulness of FFT and spectral analysis for diagnosis needs to be confirmed but seems possible.
- If prior conditions are known, then supervised learning can be used to create machine learning algorithms. Unsupervised learning needs to be further researched.

6.1 Recommendations

Volvo should implement vibration monitoring as a complement to traditional methods. By trial-and-error computerized models can be built and deployed. Trial-and-error is done by collecting new data and then comparing the real condition to what can be concluded from that vibration data. The comparison can be made manually by comparing new measurements to old measurements like in this thesis, or by setting RMS/PSD/FFT alarm-levels based on previously measured ‘bad’ conditions. After this the next step is to implement vibration analysis and have it run independently, possibly using machine learning algorithms. Similar implementations are being done in for example the paper industry or for gas and oil extraction, these might serve as inspiration.

During trial-and-error, the way all vibrational measures are calculated should also be revised to guarantee no information is lost. This includes revising the interval for RMS-calculations and choosing if PSD/FFT peaks should be taken at a few set frequencies instead of extracting the 25 first peaks as in this thesis.

To make the best of predictive maintenance, vibration analysis should be combined with process-parameters and quality outputs etc. on a company-wide scale to make best practise of predictive maintenance. However, this should be the goal and not the next step for Volvo.

6.2 Future thesis work

Future work should be mainly focused around the implementation of condition monitoring using vibration analysis. This includes:

- Implementing computerized monitoring, perhaps with machine learning. Implementation might be done by creating a machine learning model for fault detection using the analysis results of this thesis. This may also include building a model that can be used for diagnosis provided that any assumptions regarding diagnosis found in this thesis, are confirmed.
- Establish guidelines for using and interpreting results.
- Finding ways to store data.
- Try implementation on other mechanical presses than the two analysed in this thesis.

Also:

- Investigating the influence of measuring vibrations whilst producing different products.
- Investigating how features are calculated.

References

[1] Volvo Car Corporation, ”About Volvo Cars: Company,” 16 January 2018. [Online]. Available: https://group.volvocars.com/company.

[2] R. Halicioglu, L. C. Dulger och A. T. Bozdana, ”Mechanisms, classifications, and applications of servo presses: A review with comparisons.,” *Proceedings of the Institution of Mechanical Engineers Part B Journal of Engineering Manufacture,* nr September, pp. 1-18, 2015.

[3] Tooling U-SME, ”Sheet Metal Stamping Presses,” Youtube, 19 06 2014. [Online]. Available: https://www.youtube.com/watch?v=Fy_czoSfbRE. [Used 28 01 2019].

[4] D. Cattell, ”Stamping 101: Anatomy of a Mechanical Press,” 15 01 2008. [Online]. Available: https://www.thefabricator.com/article/stamping/stamping-101-anatomy-of-a-mechanical-press. [Used 28 01 2019].

[5] C. Scheffer och P. Girdhar, Practical Machinery Vibration Analysis and Predictive Maintenance, Newnes, 2004.

[6] R. K. Mobley, An Introduction to Predictive Maintenance, New York: Butterworth-Heinemann, 2002.

[7] IIT ROORKEE, ”NPTEL: Vibration Control - Chapter 37: Vibration Measurement Techniques: Basics,” 22 11 2013. [Online]. Available: https://nptel.ac.in/courses/112107088/37. [Used 24 01 2019].

[8] National Instruments, ”Measuring Vibration with Accelerometers,” National Instruments, 14 12 2017. [Online]. Available: http://www.ni.com/white-paper/3807/en/. [Used 28 01 2019].

[9] E. Källström, ”Data Driven Condition Monitoring for Transmission and Axles,” Luleå University of Technology, Luleå, 2018.

[10] X. Tian, ”Enhanced information extraction from noisy vibration data for machinery fault detection and diagnosis (pp. 26-31),” University of Huddersfield Repository, Huddersfield, 2017.

[11] Swedish Standards Institute, *SVENSK STANDARD SS-ISO 10816-3:2009: Mechanical vibration – Evaluation of machine vibration by measurements on non-rotating parts – Part 3: Industrial machines with nominal power above 15 kW and nominal speeds between 120 r/min and 15 000 r/min when measu,* Stockholm: SIS Förlag AB, 2009.

[12] M. P. Norton och D. G. Karczub, ”Chapter 8: Noise and vibration as a diagnostic tool,” i *Fundamentals of Noise and Vibration Analysis for Engineers*, Cambridge, UK, Cambridge University Press, 2003, pp. 488-563.

[13] C. Prof. Costa, ”Review of Vibration Analysis Techniques: Chapter 4,” [Online]. Available:

http://professorcesarcosta.com.br/upload/imagens_upload/Review_Of_Vibration_Analysis_Techniques_05chapter4.pdf. [Used 17 04 2019].

[14] J. Dai, P. Chen C.L, X.-Y. Xu och P. Hu, ”Condition Monitoring on Complex Machinery for Predictive Maintenance and Process Control,” i *2008 IEEE International Conference on Systems, Man and Cybernetics* , Singapore, 2008.

[15] G. E. Hearn och A. V. Metcalfe, 5 - Frequency representation of random signals, Butterworth-Heinemann, 1995, pp. 130-132.

[16] D. Davies, ”RMS From Time History And FFT Spectrum,” Prosig Noise & Vibration Blog, 06 01 2015. [Online]. Available: http://blog.prosig.com/2015/01/06/rms-from-time-history-and-fft-spectrum/. [Used 03 03 2019].

[17] Vibration Research Corp., ”What is the PSD?,” Vibration Research Corp., 2017. [Online]. Available: http://vru.vibrationresearch.com/lesson/what-is-the-psd/. [Used 24 04 2019].

[18] Hewlett-Packard Co, ”The Fundamentals of Signal Analysis,” Hewlett-Packard Co, 1994.

[19] G. P. Brian och K. Starry, ”Rolling Element Bearing Analysis,” The American Society for Nondestructive Testing Inc. , 2011.

[20] I. Ubhayaratnea, M. Pereira. P, Y. Xiang och B. Rolfe. F, ”Audio signal analysis for tool wear monitoring in sheet metal stamping,” *Mechanical Systems and Signal Processing,* vol. 85, p. 809–826, 2017.

[21] Volvo Cars, ”Volvo Torslanda övervakar kulskruvar med Intellinova Parallel MB,” Svensk Verkstad, 23 01 2019. [Online]. Available: http://www.svenskverkstad.se/volvo-torslanda-overvakar-kulskruvar-med-intellinova-parallel-mb?utm_source=Svensk+Verkstads+Nyhetsbrev&utm_campaign=3aa2a79b2a-EMAIL_CAMPAIGN_2017_04_24_COPY_01&utm_medium=email&utm_term=0_754e5b470a-3aa2a79b2a-42600421. [Used 29 01 2019].

[22] SPM Instrument AB, ”Södra Cell Mönsterås chooses Intellinova Parallel EN for online monitoring of chippers,” SPM Instrument AB, 10 04 2018. [Online]. Available: https://www.spminstrument.com/News/2018/Sodra-Cell-Monsteras-chooses-Intellinova-Parallel-EN-for-online-monitoring-of-chippers/. [Used 10 05 2019].

[23] SPM Instrument AB, ”Södra Cell Värö pulp mill ensures availability of drying machine with online monitoring for Industry 4.0,” SPM Instrument AB, 11 12 2018. [Online]. Available: https://www.spminstrument.com/News/2018/Sodra-Cell-Varo-pulp-mill-ensures-availability-of-drying-machine-with-online-monitoring-for-Industry-40/. [Used 10 05 2019].

[24] The Mathworks, Inc, ”Machine Learning with MATLAB, Section 1: Introducing Machine Learning,” The Mathworks, Inc, 2016.

[25] The Mathworks, Inc, ”Overcoming Four Common Obstacles to Predictive Maintenance with MATLAB and Simulink,” The Mathworks, Inc, 2018.

[26] M. Ulusoy och Mathworks, ”Predictive Maintenance, Part 2: Feature Extraction for Identifying Condition Indicators,” 2018. [Online]. Available: https://se.mathworks.com/videos/predictive-maintenance-part-2-feature-extraction-for-identifying-condition-indicators-1547125501847.html. [Used 08 03 2019].

[27] Z. Liu och Y. Guo, ”A hybrid approach to integrate machine learning and process mechanics for the prediction of specific cutting energy,” *CIRP Annals - Manufacturing Technology,* nr 67, pp. 57-60, 2018.

[28] The Mathworks, Inc, ”Baker Hughes Develops Predictive Maintenance Software for Gas and Oil Extraction Equipment Using Data Analytics and Machine Learning,” The Mathworks, Inc, [Online]. Available: https://se.mathworks.com/company/user_stories/baker-hughes-develops-predictive-maintenance-software-for-gas-and-oil-extraction-equipment-using-data-analytics-and-machine-learning.html?s_tid=OIT_19220. [Used 18 02 2019].

Appendix A

Content of Appendix A table 1 and Appendix A table 2, is from chapter 5 *"Machinery fault diagnosis using vibration analysis"* in the book "*Practical Machinery Vibration Analysis and Predictive Maintenance"* [5] by Cornelius Scheffer and Paresh Girdhar.

Appendix A table 1. Spectral components (peaks) corresponding to common faults.

Fault	**Spectral component/-s**	**Comment**
Unbalance	1x	Amplitude varies proportional to square of speed
Eccentric rotor	1x	Dominating peak corresponding to rpm of eccentric component
Bent Shaft	1x, 2x	If 1x-peak is dominant the bend is near shaft centre. If 2x-peak is dominant the bend is near shaft end
Angular misalignment	1x, 2x (also 3x)	Severe misalignment may cause higher order harmonics (3x to 8x)
Parallel misalignment	1x, 2x (also 3x)	2x is predominant. Severe misalignment may cause higher order harmonics (3x to 8x)
Internal assembly looseness	0.5x, 1x, 1.5x, 2x, 2,5x, 3x, etc.	Looseness often causes sub-harmonic multiples, e.g. ½x, 1½x, 2½x. 2x is predominant.
Looseness machine-to-baseplate	0.5x, 1x, 2x, 3x, etc.	2x is predominant
Structure looseness	1x	

Rotor rub	0.5x, 1x, 1.5x, 2x (resonance), 2,5x, 3x, etc.	1x is predominant when the shaft rpm is less than the critical shaft speed. Sub-harmonic multiples (1/4x, 1/3x, etc.) increase as the running speed increases.
High clearance in journal bearings	1x, 2x, 3x, etc.	Severely damaged bearings may have harmonics up to 10x-20x. Similar spectrum to mechanical looseness
Rolling elements bearings (4 stages)	*See details in Appendix A table 2*	*See details in Appendix A table 2*
Gear tooth wear	GMF* sidebands, excited natural gear frequencies	Increase of amplitude in the GMF sidebands, spaced by the worn tooth running speed
Gear eccentricity + backlash	High amplitude GMF sidebands, excited natural gear frequencies	
Gear misalignment	2x GMF with sidebands	Second order GMF harmonic often has higher amplitude than 1x GMF
Gear tooth crack	1x, excited natural gear frequencies	Recognizable as spikiness in the time domain signal
Belt – worn/loose/mismatched	1-4x belt frequency	Belt frequency is subharmonic and can be calculated as: (Pi x pulley rpm x pitch diameter) / belt length

Belt/sheave misalignment	1x driver/driven	Corresponding rpm depends on the measurement position
(Belt) eccentric sheave	1x sheave rpm	
Belt resonance	1x rpm with resonance peak close to 1x	May cause harmonics
Rotor cracked or broken (electrical)	1x with pole pass frequency sidebands	
Eccentric rotor (electrical)	1x, 2x, 3x, 4x etc. with pole pass frequency (F_p)** sidebands	
Loose rotor bar (electrical)	2x and rotor bar pass frequency with harmonic sidebands	rotor bar pass frequency (RBPF) = number of rotor bars x rpm
Stator defects (electrical)	1x, $2F_L$**, with F_p sidebands	
Phasing issues (electrical)	$2F_L$ with $1/3F_L$ sidebands	

**Gear Mesh Frequency (GMF) = number of teeth on pinion x pinion rpm*

*** F_L = electrical line frequency*

F_S = slip frequency = $(2 \times F_L) / P$ - rpm

F_P = pole pass frequency = $F_S \times P$

P = number of poles

Appendix A table 2. Spectral components corresponding to different levels of wear in rolling element bearings.

Level of wear	Spectral component/-s	Comment
Stage 1. No visible defects to bearing, raceway may appear dull.	Indications in the ultrasonic frequency ranges (~20-60 kHz /120-360 krpm)	Uses high-frequency detection techniques.

Stage 2. Minute pits in raceway	Peaks in ~5-20 kHz / 30-120 krpm, with possible sidebands with rpm spacing	Peaks that show up with high frequency detection may have doubled in amplitude compared to stage 1.
Stage 3. Larger and more visible pits in raceway extending towards the raceway edge. Bearing should be replaced at this stage.	Peaks at BPFO** and BPFI** with harmonics and sidebands. Also, high frequency peaks.	Peaks that show up with high frequency detection may have doubled in amplitude compared to stage 2.
Stage 4. Pits and wear merge together creating a smoother surface but with high clearance. The bearing will become hot and noisy. May break and cause serious damage if not proper action is taken.	RPM harmonics 1x, 2x, 3x will increase. A noise floor in the form of a haystack of random high frequency vibrations will appear. Ultra-high frequencies may lesser at the end of stage 4.	The amplitude of the broad band of noise will initially be large but then decrease inly to increase again near to failure.

**Zone A: machine rpm and harmonics zone*

Zone B: bearing defect frequencies zone (5-30 krpm)

Zone C: beating component natural frequencies zone (30-120 krpm)

Zone D: high-frequency-detection (HFD) zone (beyond 120 krpm).

***BPFI – Ball Pass Frequency – Inner*

BPFO – Ball Pass Frequency – Outer